NASA TECHNICAL NOTE

NASA TN D-4754

NASA TN D-4754

EQUILIBRIUM NORMAL-SHOCK AND STAGNATION-POINT PROPERTIES OF HELIUM FOR INCIDENT-SHOCK MACH NUMBERS FROM 1 TO 30

by Walter B. Olstad, Jane T. Kemper, and Roger D. Bengtson

Langley Research Center
Langley Station, Hampton, Va.

NATIONAL AERONAUTICS AND SPACE ADMINISTRATION • WASHINGTON, D. C. • SEPTEMBER 1968

NASA TN D-4754

EQUILIBRIUM NORMAL-SHOCK AND STAGNATION-POINT PROPERTIES OF HELIUM FOR INCIDENT-SHOCK MACH NUMBERS FROM 1 TO 30

By Walter B. Olstad, Jane T. Kemper, and Roger D. Bengtson

Langley Research Center
Langley Station, Hampton, Va.

NATIONAL AERONAUTICS AND SPACE ADMINISTRATION

For sale by the Clearinghouse for Federal Scientific and Technical Information
Springfield, Virginia 22151 – CFSTI price $3.00

EQUILIBRIUM NORMAL-SHOCK AND STAGNATION-POINT PROPERTIES OF HELIUM FOR INCIDENT-SHOCK MACH NUMBERS FROM 1 TO 30

By Walter B. Olstad, Jane T. Kemper, and Roger D. Bengtson
Langley Research Center

SUMMARY

Charts are presented of the thermodynamic properties of helium, including the effects of ionization and particle interactions, for temperatures to 100 000° K and pressures from 10^{-7} to 10^{4} atmospheres. The properties behind the incident, standing, and reflected shocks and at the in-flight and shock-tube stagnation conditions are also presented for incident-shock Mach numbers from 1 to 30 and quiescent gas pressure from 10^{-7} to 1 atmosphere.

INTRODUCTION

Helium has been used extensively in research facilities such as hypersonic wind tunnels, where it serves as the test medium, and in shock tubes, in which it is used as the driver gas. The perfect gas relations for helium at Mach numbers from 1 to 30 were presented in reference 1. Arave (ref. 2) presented the equilibrium flow properties for helium including the effect of first ionization for Mach numbers from 14 to 30 and quiescent gas pressures of 10, 1, and 0.1 millimeters of mercury at a quiescent gas temperature of 300° K. The quiescent gas is that gas, upstream of the incident shock, which is at rest with respect to the laboratory. With the advent of the expansion tube (ref. 3), it became necessary to know the equilibrium hypersonic flow properties of helium corresponding to quiescent gas pressures as low as 10^{-7} atmosphere. The present work was undertaken to satisfy this need and to include the effects of second ionization and particle interactions.

Charts are presented of the thermodynamic properties of helium for temperatures to 100 000° K and pressures from 10^{-7} to 10^{4} atmospheres. The properties behind the incident, standing, and reflected shocks and at the in-flight and shock-tube stagnation conditions are also presented for incident-shock Mach numbers from 1 to 30, quiescent gas pressures from 10^{-7} to 1 atmosphere, and a quiescent gas temperature of 300° K. In-flight stagnation conditions result from an isentropic compression which brings the flow to rest, relative to the laboratory (or an object flying in an atmosphere), downstream

of the incident shock. Shock-tube stagnation conditions result from an isentropic compression which brings the flow to rest, relative to the laboratory, downstream of the standing shock.

SYMBOLS

a	speed of sound, centimeters/second
a_o	radius of first Bohr orbit, 5.292×10^{-9} centimeter; speed of sound at p_o and T_o, 97 242 centimeters/second
$B(i)$	electronic partition function of ith component
c_p, c_v	specific heats, at constant pressure and constant volume, respectively, ergs/mole-^oK
E	energy per unit mass or per original mole of nonionized gas, ergs/gram
$E(i)$	energy per unit mass or per original mole of ith component, ergs/gram
$E_n(i)$	energy of nth electronic level of ith component, ^oK
e	charge of electron, 4.80286×10^{-10} electrostatic unit
$g_n(i)$	degeneracy of nth electronic level of ith component
H	enthalpy per unit mass or per original mole of nonionized gas, ergs/gram
h	Planck constant, 6.62517×10^{-27} erg-seconds
I^+, I^{++}	ionization potential for neutral and singly ionized atoms, ^oK
k	Boltzmann constant, 1.38044×10^{-16} erg/^oK
M	Mach number
m_k	mass of particle of kth component, $m_e = 9.1083 \times 10^{-28}$ gram and $m_{He} = m_{He^+} = m_{He^{++}} = 6.6478 \times 10^{-24}$ gram

$K_{p,j}$	equilibrium constant of jth reaction, dynes/centimeter^2
N(i)	number density of ith component, centimeter^{-3}
n	integer indicating electronic level
n_i	quantum number for electronic energy levels of ith component
n_i^*	limiting quantum number for electronic energy levels of ith component
p	pressure, dynes/centimeter^2
p_o	reference pressure, 1 atmosphere $(1.01325 \times 10^6$ dynes/centimeter$^2)$
p_{coul}	pressure-correction term accounting for electrostatic forces, dynes/centimeter^2
Q(i)	partition function of ith component
R	gas constant, 3.32824×10^8 ergs/mole-^oK
$r_{o,z}$	average distance from nucleus to nearest ion with charge ze, centimeters
s	entropy per unit mass or per original mole of nonionized gas, ergs/mole-^oK
T	absolute temperature, ^oK
T_o	reference temperature, 273.16 ^oK
U_r	reflected-shock speed, centimeters/second
U_s	incident-shock speed, centimeters/second
u	gas velocity, centimeters/second
$\bar{u}_2$	gas velocity relative to incident shock, $U_s - u_2$, centimeters/second
$w_{i,n}$	weighting factor

X(i)	mole fraction of ith component
Z	compressibility factor
z	integer indicating charge in units of e
α	moles of He^{+} per original mole of nonionized gas
β	moles of He^{++} per original mole of nonionized gas
γ	ratio of specific heats, c_p/c_v
$\Delta\epsilon^{+},\Delta\epsilon^{++}$	ionization-potential correction terms accounting for electrostatic interactions, ^{o}K
ρ	density, grams/centimeter^3
ρ_o	density at p_o and T_o, 1.7859×10^{-4} gram/centimeter^3

Subscripts:

1	conditions ahead of incident shock $(T_1 = 300^{o}$ K; p_1 as indicated$)$
2	conditions behind incident shock
3	conditions behind standing shock in shock tube
R	conditions behind reflected shock
sf	in-flight stagnation conditions
st	shock-tube stagnation conditions

ANALYSIS

The thermodynamic properties of helium were determined from statistical mechanics in the same manner (with one relatively minor exception which is discussed subsequently) as reference 4. The reader is referred to this reference for all details. A compendium of the pertinent equations and spectroscopic constants (obtained from

ref. 5) is presented in appendix A. These equations were programmed in FORTRAN IV language for solution on the IBM 7094 electronic data processing system. The computer program called for temperature and pressure as input parameters and provided as output the following quantities: density, compressibility, mole fractions of individual species, energy, enthalpy, entropy, specific heats at constant volume and pressure, speed of sound, and the Debye-Hückel pressure correction.

The only difference between the properties presented in reference 4 and those presented herein is a result of a slightly different treatment of the effect of particle interactions on the ionization potentials of the atom and singly charged ion. In the present work the lowering of the ionization potentials as predicted by Unsöld's theory (refs. 6 and 7) is given by

$$\Delta\epsilon^{+} = \frac{157\,800}{(n_1^*)^2},\ ^{o}K \tag{1}$$

and

$$\Delta\epsilon^{++} = \frac{631\,400}{(n_2^*)^2},\ ^{o}K \tag{2}$$

for first and second ionization, respectively. The principal quantum numbers at which the combined potential of the nucleus and the nearest ion reaches a maximum were obtained from the equations

$$\frac{1}{(n_1^*)^2} = \frac{3.33a_o}{r_{o,1}} + \frac{4.3a_o}{r_{o,2}} \tag{3}$$

and

$$\frac{1}{(n_2^*)^2} = \frac{2.44a_o}{r_{o,1}} + \frac{3a_o}{r_{o,2}} \tag{4}$$

where a_o is the radius of the first Bohr orbit $(5.292 \times 10^{-9}\ \text{cm})$ and $r_{o,z}$ is the average distance from the nucleus to the nearest ion with charge ze. The average distances were given approximately by Unsöld

$$r_{o,1} = 0.62\left[N(He^{+})\right]^{-1/3},\ \text{cm} \tag{5}$$

and

$$r_{o,2} = 0.62\left[N(He^{++})\right]^{-1/3},\ \text{cm} \tag{6}$$

Here $N(He^+)$ and $N(He^{++})$ are the average number of particles of the species He^+ and He^{++}, respectively, per unit volume. Lick and Emmons in reference 4 approximated the foregoing set of formulas by the expressions

$$\Delta\epsilon^+ = 5.65 \times 10^{-3}\left[N(e^-)\right]^{1/3}, \text{ cm}^{-1} \tag{7}$$

and

$$\Delta\epsilon^{++} = 8.96 \times 10^{-3}\left[N(e^-)\right]^{1/3}, \text{ cm}^{-1} \tag{8}$$

where $N(e^-)$ is the electron density. Because of the approximate formulation of the effect of particle interactions on the ionization potentials, there is little to recommend the choice of one calculation over the other.

The program for the equilibrium thermodynamic properties of helium was combined with the program for calculation of normal-shock and stagnation-point conditions described in reference 8. With the two programs coupled, it was possible to compute the conditions behind an incident shock (a shock moving into a quiescent gas), a standing shock (a bow shock in front of a stationary body after passage of an incident shock), and a reflected shock (the reflection of an incident shock from a stationary, perpendicular surface) as well as the isentropic stagnation conditions upstream and downstream of a standing shock.

A brief summary of the normal-shock equations is presented in appendix B.

PRESENTATION OF RESULTS

The thermodynamic properties of helium are presented as functions of temperature (to 100 000° K) and pressure (from 10^{-7} to 10^4 atm) in figures 1 to 11. Values of the Debye-Hückel pressure correction p_{coul}/p_o for helium are given in the following table:

T, °K	Value of p_{coul}/p_o for –			
	$p/p_o = 10^{-2}$	$p/p_o = 10^0$	$p/p_o = 10^2$	$p/p_o = 10^4$
10×10^3	5.08×10^{-8}	5.11×10^{-6}	5.16×10^{-4}	5.27×10^{-2}
20	3.12×10^{-6}	2.33×10^{-3}	3.95×10^{-1}	4.77×10^{-1}
30	1.37	1.35	1.33×10^0	3.83×10^2
40	8.65×10^{-7}	7.83×10^{-4}	7.83×10^{-1}	6.39
50	5.33	5.60	5.00	5.14
60	3.70	3.74	3.77	3.57
70	2.72	2.72	2.85	2.69
80	2.08	2.08	2.13	2.16
90	1.64	1.64	1.66	1.74
100	1.33	1.33	1.34	1.40

The values of the pressure-correction term are always small in the range of temperatures and pressures covered by the shock-tube calculations and, consequently, have been neglected in these calculations.

The flow properties behind the incident, standing, and reflected shocks and at the in-flight and shock-tube stagnation points are presented in figures 12 to 28 for incident-shock Mach numbers from 1 to 30, quiescent gas pressures from 10^{-7} to 1 atmosphere, and a quiescent gas temperature of 300° K.

All curves presented in the figures were plotted by a plotter which draws a straight line between succeeding data points.

SUMMARY OF RESULTS

The thermodynamic properties presented herein are in good agreement with the less extensive results of reference 4. The largest differences, which are caused by the slightly different treatment of particle interactions, occur at the largest values of temperature and pressure considered in reference 4. For example, at a temperature of $50\,000^{\circ}$ K and a pressure of 10^3 atmospheres, the difference in the mole fraction of free electrons between the present report and reference 4 is about 0.003, or less than 1 percent.

The flow properties behind the incident, standing, and reflected shocks as well as at the in-flight and shock-tube stagnation points agree well with the more limited results presented in reference 2 except at the upper limit of the incident-shock Mach number range, where second ionization (not accounted for in ref. 2) becomes important.

Langley Research Center,
National Aeronautics and Space Administration,
Langley Station, Hampton, Va., April 25, 1968,
129-01-03-07-23.

APPENDIX A

THERMODYNAMIC PROPERTIES OF HELIUM

The equations used in the calculations for the thermodynamic properties are presented in this appendix.

Partition Functions

The partition functions per particle for the individual species are

$$\left.\begin{aligned} Q(He) &= \left(\frac{2\pi m_{He}}{h^2}\right)^{3/2} \frac{(kT)^{5/2}}{p} B(He) \\ Q(He^+) &= \left(\frac{2\pi m_{He^+}}{h^2}\right)^{3/2} \frac{(kT)^{5/2}}{p} B(He^+) e^{-I^+/T} \\ Q(He^{++}) &= \left(\frac{2\pi m_{He^{++}}}{h^2}\right)^{3/2} \frac{(kT)^{5/2}}{p} e^{-(I^+ + I^{++})/T} \\ Q(e^-) &= 2\left(\frac{2\pi m_e}{h^2}\right)^{3/2} \frac{(kT)^{5/2}}{p} \end{aligned}\right\} \tag{A1}$$

where

$$\left.\begin{aligned} B(He) &= \sum_{n=1}^{n_1} w_{1,n} g_n(He) e^{-E_n(He)/T} \\ B(He^+) &= \sum_{n=1}^{n_2} w_{2,n} g_n(He^+) e^{-E_n(He^+)/T} \end{aligned}\right\} \tag{A2}$$

with

$n_1 = 8$, if $n_1^* \geqq 7$

n_1 equal to the largest integer less than $(n_1^* + 1)$, if $n_1^* < 7$

$n_2 = 7$, if $n_2^* \geqq 6$

APPENDIX A

n_2 equal to the largest integer less than $(n_2^* + 1)$, if $n_2^* < 6$

$w_{i,n} = 1.0$, if $n \leqq n_i^*$, for i equal to 1 or 2

and

$w_{i,n} = n_i - n_i^*$, if $n = n_i > n_i^*$, for i equal to 1 or 2

Also,

$$\left.\begin{aligned} I^+ &= 285\,287 - \Delta\epsilon^+ \\ I^{++} &= 631\,400 - \Delta\epsilon^{++} \end{aligned}\right\} \tag{A3}$$

The reductions in the ionization potentials are obtained from the equations

$$\left.\begin{aligned} \Delta\epsilon^+ &= \frac{157\,800}{(n_1^*)^2} \\ \Delta\epsilon^{++} &= \frac{631\,400}{(n_2^*)^2} \end{aligned}\right\} \tag{A4}$$

where

$$\left.\begin{aligned} \frac{1}{(n_1^*)^2} &= \frac{3.33a_o}{r_{o,1}} + \frac{4.3a_o}{r_{o,2}} \\ \frac{1}{(n_2^*)^2} &= \frac{2.44a_o}{r_{o,1}} + \frac{3a_o}{r_{o,2}} \end{aligned}\right\} \tag{A5}$$

in which

$$\left.\begin{aligned} r_{o,1} &= 0.62\left[N(He^+)\right]^{-1/3} \\ r_{o,2} &= 0.62\left[N(He^{++})\right]^{-1/3} \end{aligned}\right\} \tag{A6}$$

with

$$\left.\begin{aligned} N(He^+) &= 2.687 \times 10^{19} Z\left(\frac{\rho}{\rho_o}\right) X(He^+) \\ N(He^{++}) &= 2.687 \times 10^{19} Z\left(\frac{\rho}{\rho_o}\right) X(He^{++}) \end{aligned}\right\} \tag{A7}$$

APPENDIX A

Equilibrium Composition

The equilibrium constants for the two reactions

$$He \rightleftharpoons He^+ + e^-$$

and

$$He^+ \rightleftharpoons He^{++} + e^-$$

are, respectively,

$$\frac{K_{p,1}}{p} = \frac{Q(He^+)Q(e^-)}{Q(He)} = \frac{\alpha(\alpha + 2\beta)}{(1 - \alpha - \beta)(1 + \alpha + 2\beta)} \tag{A8}$$

and

$$\frac{K_{p,2}}{p} = \frac{Q(He^{++})Q(e^-)}{Q(He^+)} = \frac{\beta(\alpha + 2\beta)}{\alpha(1 + \alpha + 2\beta)} \tag{A9}$$

where

$$\left.\begin{aligned} Z &= 1 + \alpha + 2\beta \\ X(He) &= \frac{1 - \alpha - \beta}{Z} \\ X(He^+) &= \frac{\alpha}{Z} \\ X(He^{++}) &= \frac{\beta}{Z} \\ X(e^-) &= \frac{\alpha + 2\beta}{Z} \end{aligned}\right\} \tag{A10}$$

With values of $\Delta\epsilon^+$ and $\Delta\epsilon^{++}$ given, equations (A8) and (A9) can be solved simultaneously for $\alpha + 2\beta$ and the species mole fractions. Equations (A4) to (A7) can then be used to compute new values of $\Delta\epsilon^+$ and $\Delta\epsilon^{++}$. The procedure is repeated with the new values until the conditions

$$\left.\begin{aligned} \frac{\left|\Delta\epsilon^+_{k+1} - \Delta\epsilon^+_k\right|}{T} &< 10^{-5} \\ \frac{\left|\Delta\epsilon^{++}_{k+1} - \Delta\epsilon^{++}_k\right|}{T} &< 10^{-5} \end{aligned}\right\} \tag{A11}$$

are satisfied. Here the subscripts on $\Delta\epsilon^+$ and $\Delta\epsilon^{++}$ indicate the trial number.

APPENDIX A

Thermodynamic Properties of the Mixture

The thermodynamic properties of the mixture are given by the equations

$$\frac{\rho}{\rho_o} = \left(\frac{p}{p_o}\right) \Big/ Z\left(\frac{T}{T_o}\right) \tag{A12}$$

and

$$\frac{E}{RT_o} = Z\left[X(He)\frac{E(He)}{RT_o} + X\left(He^+\right)\frac{E\left(He^+\right)}{RT_o} + X\left(He^{++}\right)\frac{E\left(He^{++}\right)}{RT_o} + X\left(e^-\right)\frac{E\left(e^-\right)}{RT_o}\right] \tag{A13}$$

where

$$\frac{E(He)}{RT_o} = \frac{T}{T_o}\left[\frac{3}{2} + \frac{\sum_{n=1}^{n_1} w_{1,n}E_n(He)g_n(He)e^{-E_n(He)/T}}{TB(He)}\right] \tag{A14}$$

$$\frac{E\left(He^+\right)}{RT_o} = \frac{T}{T_o}\left[\frac{3}{2} + \frac{\sum_{n=1}^{n_2} w_{2,n}E_n\left(He^+\right)g_n\left(He^+\right)e^{-E_n\left(He^+\right)/T}}{TB\left(He^+\right)} + \frac{I^+}{T}\right] \tag{A15}$$

$$\frac{E\left(He^{++}\right)}{RT_o} = \frac{T}{T_o}\left[\frac{3}{2} + \frac{I^+ + I^{++}}{T}\right] \tag{A16}$$

$$\frac{E\left(e^-\right)}{RT_o} = \frac{3}{2}\frac{T}{T_o} \tag{A17}$$

$$\frac{H}{RT_o} = \frac{E}{RT_o} + Z\frac{T}{T_o} \tag{A18}$$

$$\frac{s}{R} = \frac{T_o}{T}\left(\frac{H}{RT_o}\right) + Z\Big\{X(He)\ \ln\left[Q(He)/X(He)\right] + X\left(He^+\right)\ \ln\left[Q\left(He^+\right)/X\left(He^+\right)\right] + X\left(He^{++}\right)\ \ln\left[Q\left(He^{++}\right)/X\left(He^{++}\right)\right] + X\left(e^-\right)\ \ln\left[Q\left(e^-\right)/X\left(e^-\right)\right]\Big\} \tag{A19}$$

$$\frac{c_p}{R} = T_o\left[\frac{\partial\left(H/RT_o\right)}{\partial T}\right]_p \tag{A20}$$

APPENDIX A

$$\frac{c_v}{R} = \frac{c_p}{R} - Z\frac{1 + (T/Z)(\partial Z/\partial T)_p}{1 + (p/Z)(\partial Z/\partial p)_T} \tag{A21}$$

$$\gamma = \frac{c_p}{c_v} \tag{A22}$$

and

$$\frac{a}{a_o} = \left(Z\frac{3\gamma T}{5T_o}\right)^{1/2}\left[1 - \left(\frac{p}{Z}\right)\left(\frac{\partial Z}{\partial p}\right)_T\right]^{-1/2} \tag{A23}$$

The derivatives $(\partial/\partial T)_p$ and $(\partial/\partial p)_T$ were evaluated numerically. The evaluation of these derivatives was necessary because of the unknown dependence of $\Delta\epsilon^+$ and $\Delta\epsilon^{++}$ on temperature and pressure. The Debye-Hückel pressure correction was obtained from the equation

$$\frac{p_{coul}}{p_o} = 7.6591 \times 10^2\left(\frac{\rho}{\rho_o}\right)^{3/2}\left(\frac{1}{T}\right)^{1/2}\left[X(e^-) + X(He^+) + 4X(He^{++})\right] \tag{A24}$$

The actual pressure is then given by

$$\frac{p}{p_o} = Z\left(\frac{\rho}{\rho_o}\right)\left(\frac{T}{T_o}\right) + \frac{p_{coul}}{p_o} \tag{A25}$$

Because the correction was always found to be small, it was not included in the normal-shock calculations of this report.

Spectroscopic Constants

The spectroscopic constants for neutral and singly ionized helium are presented in the following tables.

Neutral helium:

Electronic level n	g_n(He)	E_n(He), °K
1	1	0
2	3	230 025
3	13	243 308
4	36	267 219
5	64	275 354
6	64	278 975
7	64	280 934
8	64	282 113

Singly ionized helium:

Electronic level n	$g_n(He^+)$	$E_n(He^+)$, °K
1	2	0
2	8	473 929
3	14	561 142
4	22	592 117
5	32	606 633
6	44	614 046
7	58	618 700

APPENDIX B

NORMAL-SHOCK EQUATIONS

Incident Shock

A plane incident shock moving into a quiescent gas is shown in the following sketch:

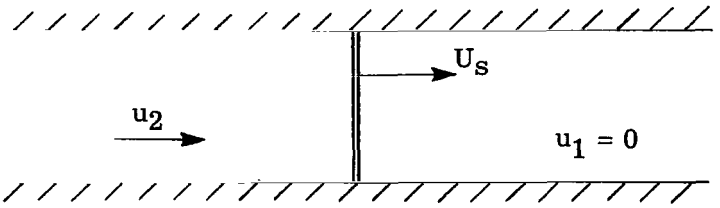

The conservation equations for the incident shock may be written as

$$\rho_2 \bar{u}_2 = \rho_1 U_s \tag{B1}$$

$$p_2 + \rho_2 \bar{u}_2^2 = p_1 + \rho_1 U_s^2 \tag{B2}$$

and

$$H_2 + \frac{1}{2}\bar{u}_2^2 = H_1 + \frac{1}{2}U_s^2 \tag{B3}$$

Equations (B1) to (B3) together with the equation of state

$$\rho_2 = \rho(p_2, H_2) \tag{B4}$$

form the system of equations for the unknowns ρ_2, p_2, and H_2.

Standing Shock

A standing shock, such as a bow shock in front of a body, is shown in the following sketch:

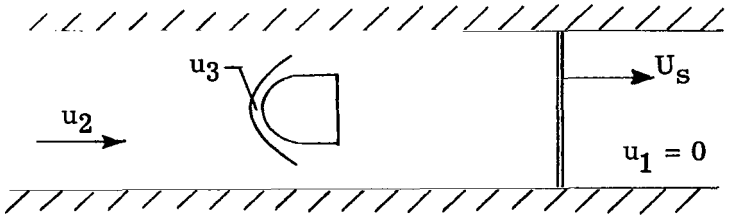

APPENDIX B

The conservation equations across the normal portion of the standing shock are

$$\rho_2 u_2 = \rho_3 u_3 \tag{B5}$$

$$p_2 + \rho_2 u_2^2 = p_3 + \rho_3 u_3^2 \tag{B6}$$

and

$$H_2 + \frac{1}{2} u_2^2 = H_3 + \frac{1}{2} u_3^2 \tag{B7}$$

The subscript 3 denotes quantities immediately downstream of the standing shock. The equation of state

$$\rho_3 = \rho(p_3, H_3) \tag{B8}$$

completes the system.

Reflected Shock

A normal shock reflected from the closed end of a (one-dimensional) tube is shown in the following sketch:

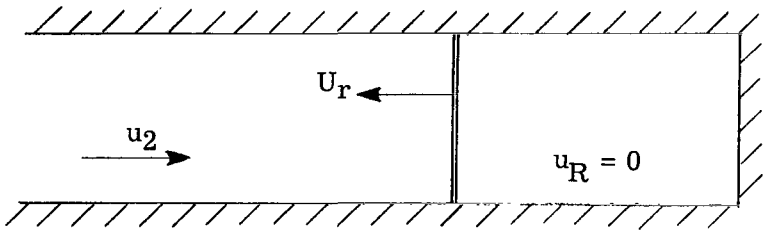

The conservation equations when written in a shock-fixed coordinate system are

$$\rho_2 (u_2 + U_r) = \rho_R U_r \tag{B9}$$

$$p_2 + \rho_2 (u_2 + U_r)^2 = p_R + \rho_R U_r^2 \tag{B10}$$

and

$$H_2 + \frac{1}{2}(u_2 + U_r)^2 = H_R + \frac{1}{2} U_r^2 \tag{B11}$$

APPENDIX B

The equation of state is used in the form

$$\rho_R = \rho(p_R, H_R) \tag{B12}$$

Stagnation Conditions

The stagnation conditions upstream of a standing shock (also called the "in-flight stagnation conditions") can be determined from the equation of state

$$\rho_{sf} = \rho(s_{sf}, H_{sf}) \tag{B13}$$

and the conditions

$$\left.\begin{aligned} H_{sf} &= H_1 + \tfrac{1}{2}U_s^2 \\ s_{sf} &= s_2 \end{aligned}\right\} \tag{B14}$$

Similarly, the stagnation conditions downstream of a standing shock (also called the "shock-tube stagnation conditions") can be determined from the equation of state

$$\rho_{st} = \rho(s_{st}, H_{st}) \tag{B15}$$

and the conditions

$$\left.\begin{aligned} H_{st} &= H_2 + \tfrac{1}{2}u_2^2 \\ s_{st} &= s_3 \end{aligned}\right\} \tag{B16}$$

The numerical procedures required to solve the equations of this and the preceding sections of this appendix are fully detailed in reference 8.

REFERENCES

1. Mueller, James N.: Equations, Tables, and Figures for Use in the Analysis of Helium Flow at Supersonic and Hypersonic Speeds. NACA TN 4063, 1957.

2. Arave, R. J.: Helium Hypersonic Flow Properties. Doc. No. D2-11721, Boeing Co., Sept. 5, 1961.

3. Trimpi, Robert L.: A Preliminary Theoretical Study of the Expansion Tube, a New Device for Producing High-Enthalpy Short-Duration Hypersonic Gas Flows. NASA TR R-133, 1962.

4. Lick, Wilbert J.; and Emmons, Howard W.: Thermodynamic Properties of Helium to 50,000° K. Harvard Univ. Press (Cambridge, Mass.), 1962.

5. Moore, Charlotte E.: Atomic Energy Levels. Vol. I - 1H-23V. NBS Circ. 467, U.S. Dept. Com., June 15, 1949.

6. Unsöld, A.: Zur Berechnung der Zustandsummen für Atome und Ionen in einem teilweise ionisierten Gas. Z. Astrophys., Bd. 24, 1948, pp. 355-362.

7. Unsöld, A.: Physik der Sternatmosphären. Zweite Aufl., Springer-Verlag (Berlin), 1955.

8. Callis, Linwood B.; and Kemper, Jane T.: A Program for Equilibrium Normal Shock and Stagnation Point Solutions for Arbitrary Gas Mixtures. NASA TN D-3215, 1966.

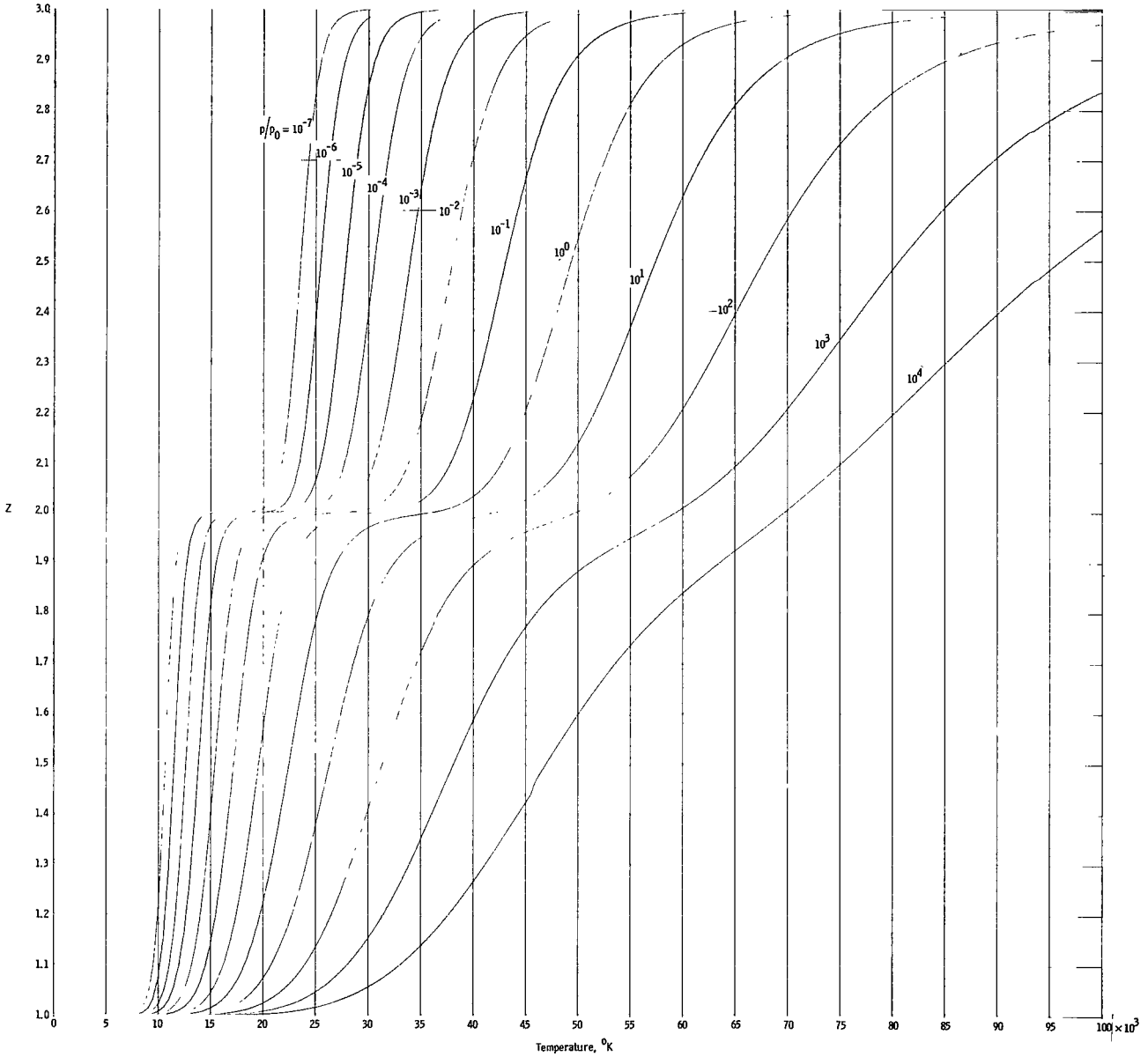

Figure 1.- Compressibility of helium.

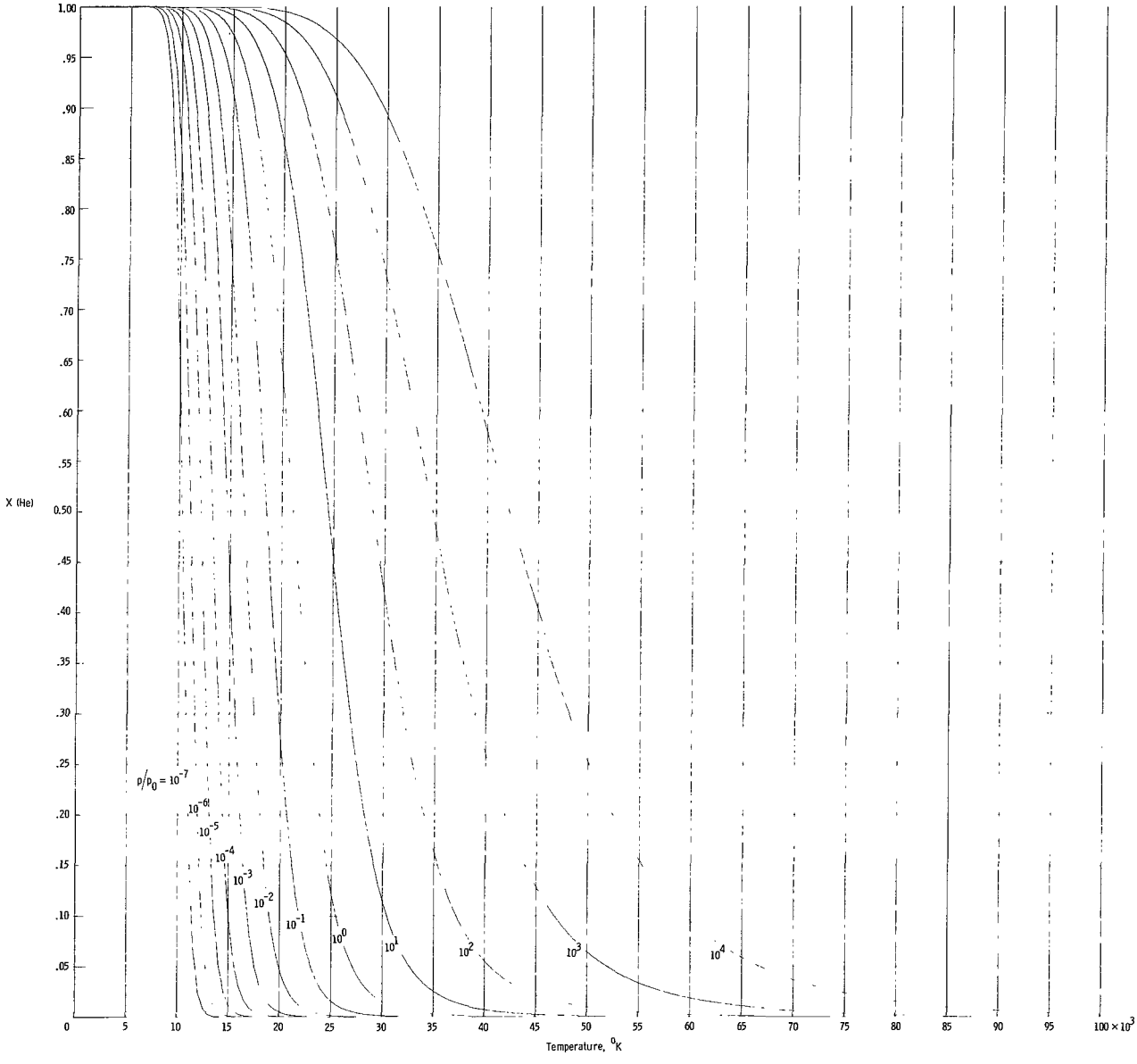

Figure 2.- Mole fraction of neutral helium.

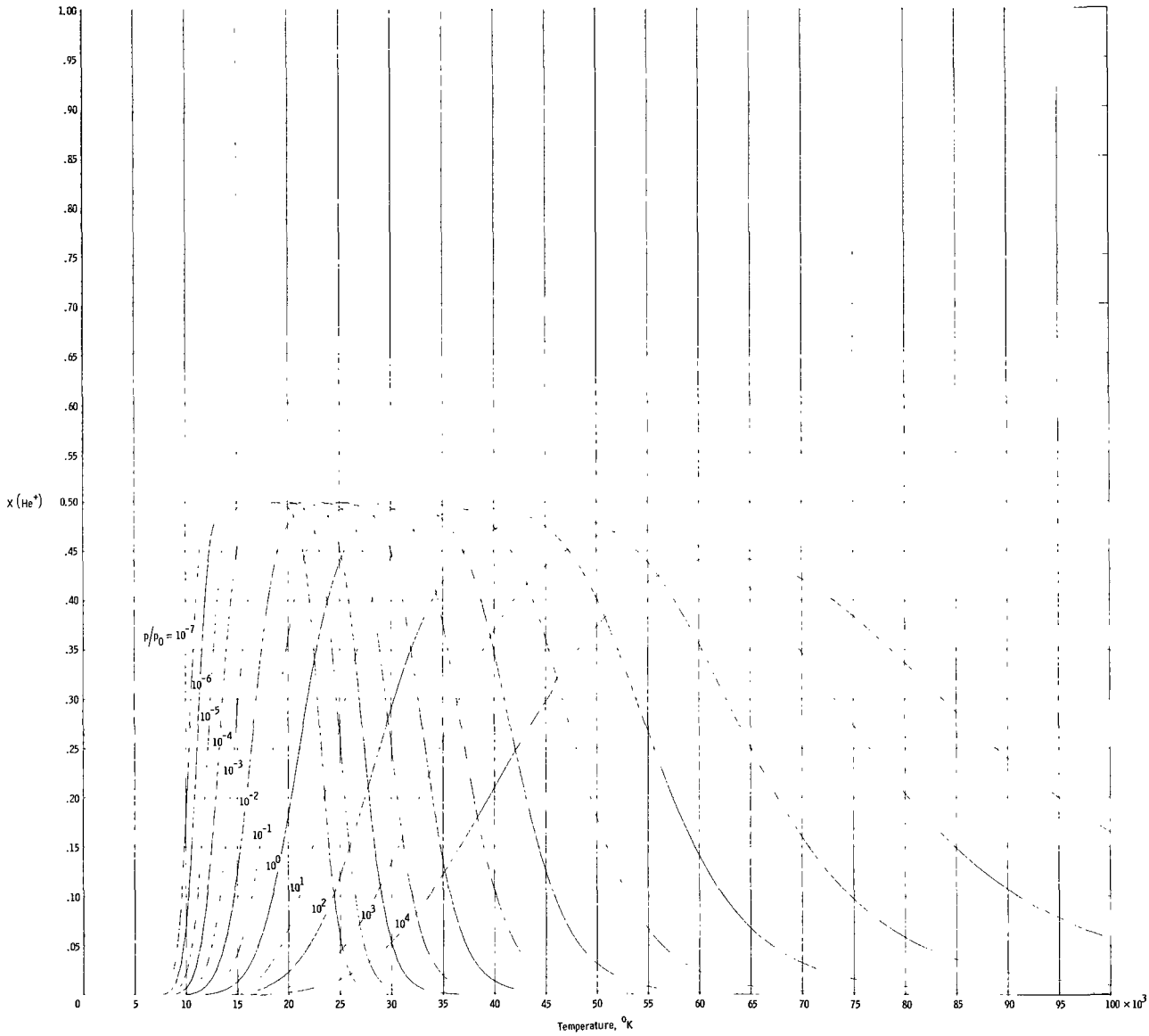

Figure 3.- Mole fraction of singly ionized helium.

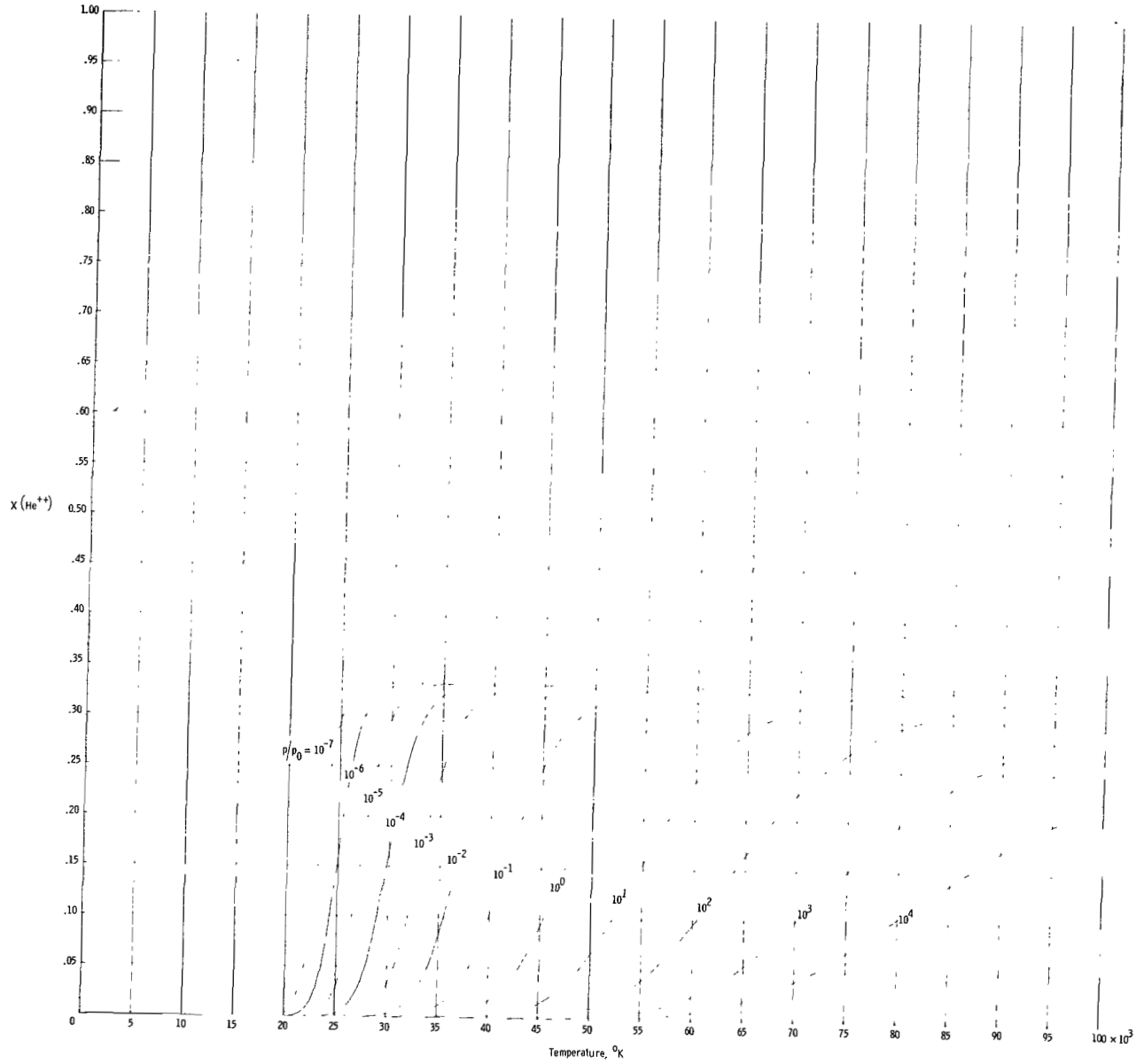

Figure 4.- Mole fraction of doubly ionized helium.

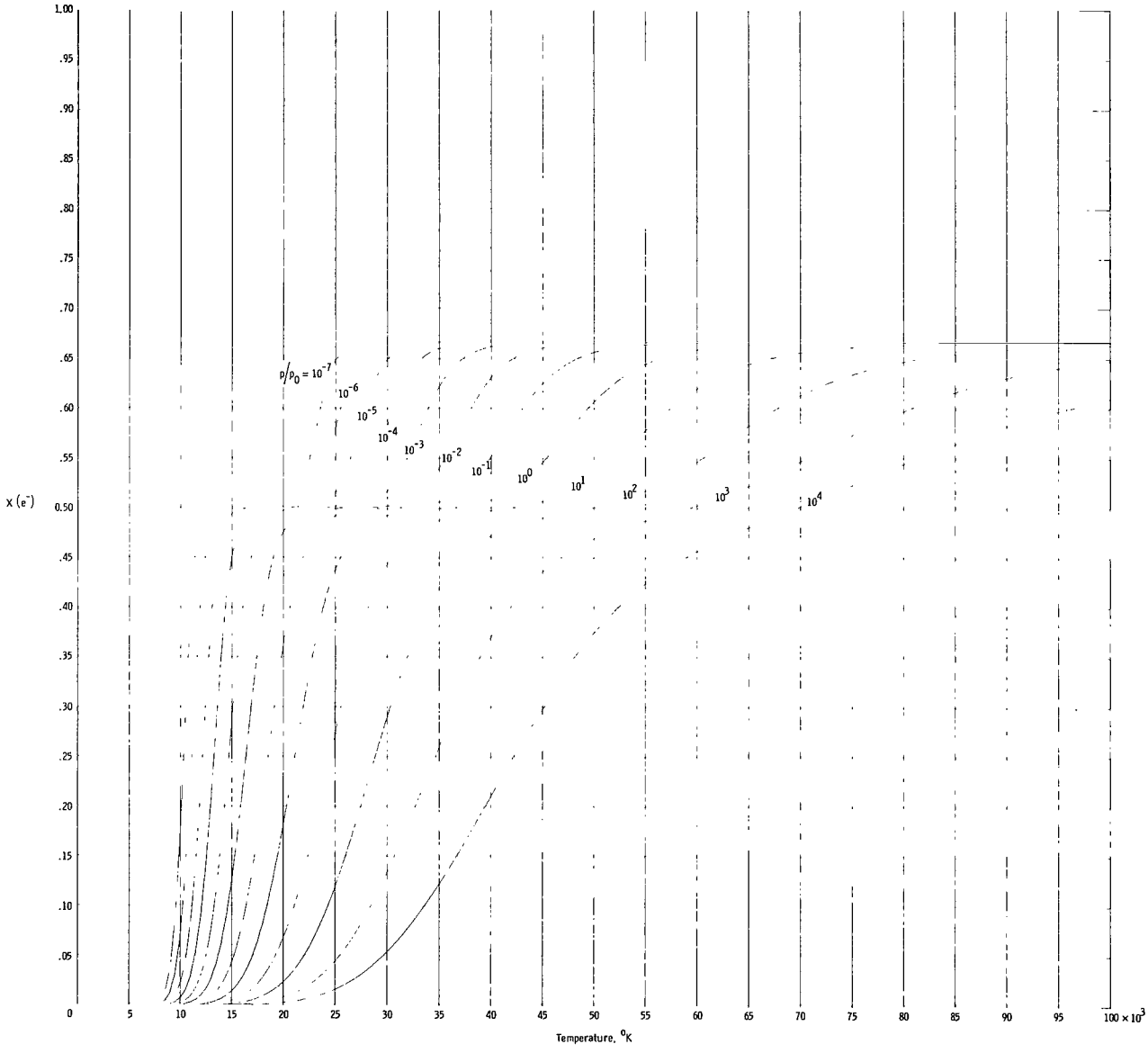

Figure 5.- Mole fraction of free electrons.

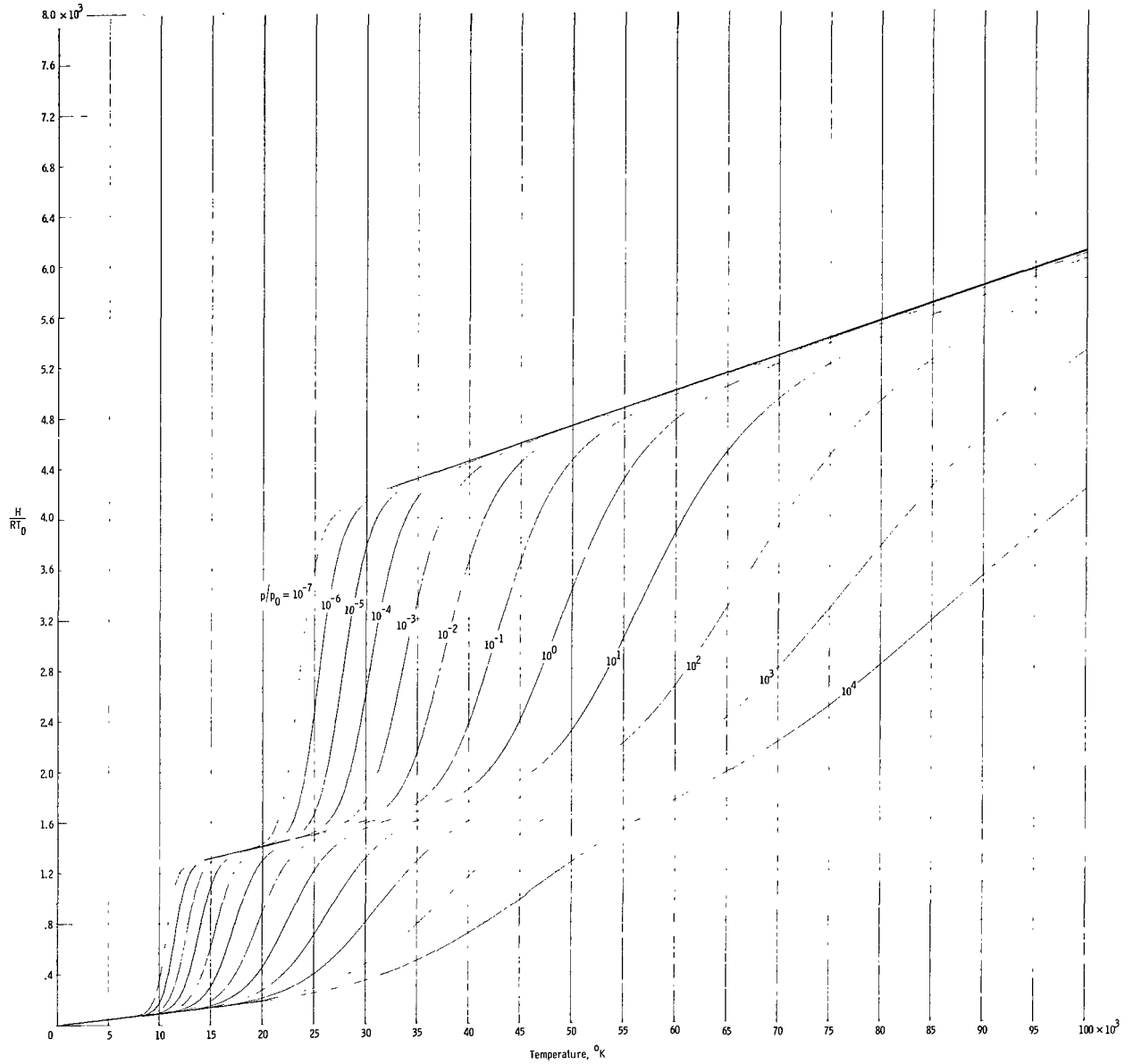

Figure 6.- Enthalpy per unit mass or per original mole of helium.

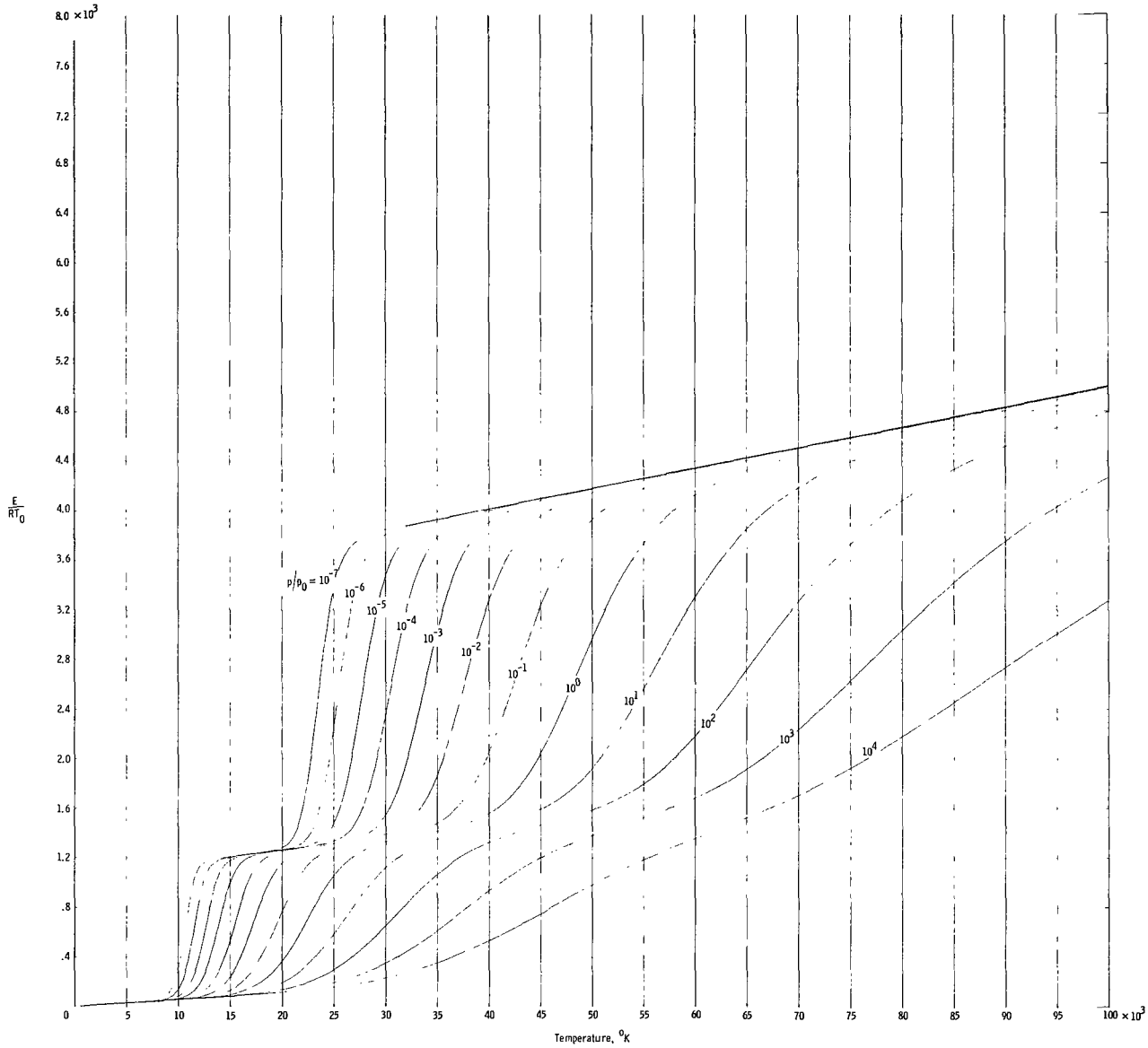

Figure 7.- Energy per unit mass or per original mole of helium.

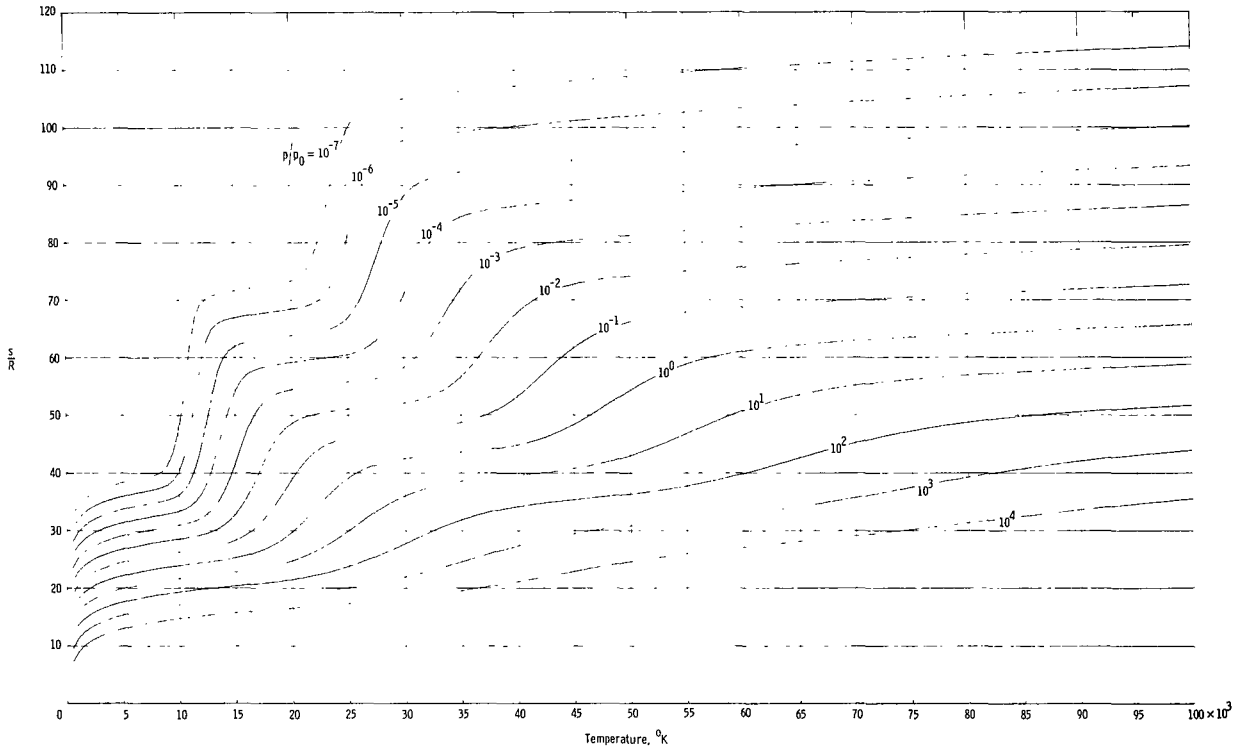

Figure 8.- Entropy per unit mass or per original mole of helium.

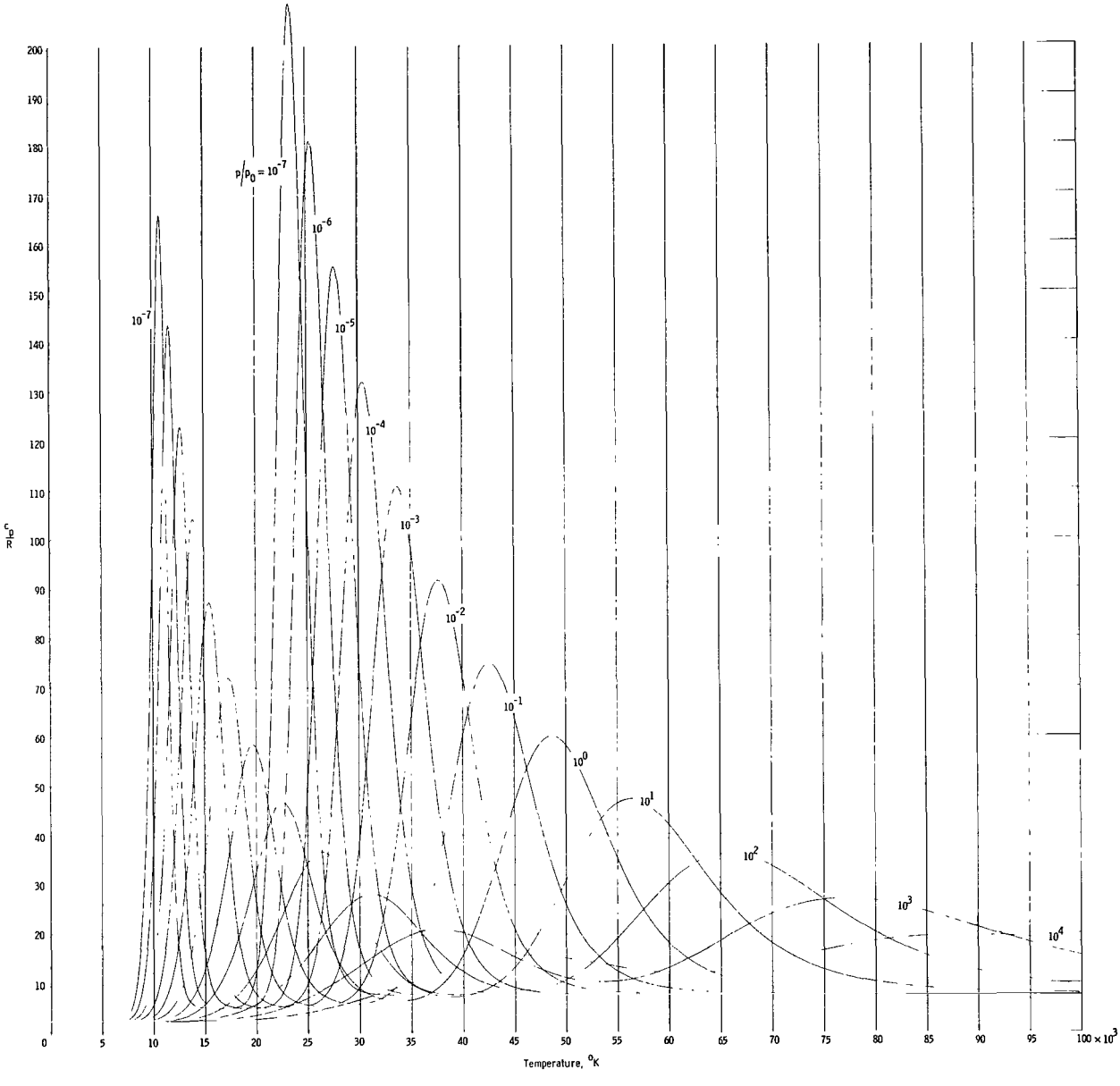

Figure 9.- Specific heat at constant pressure of helium.

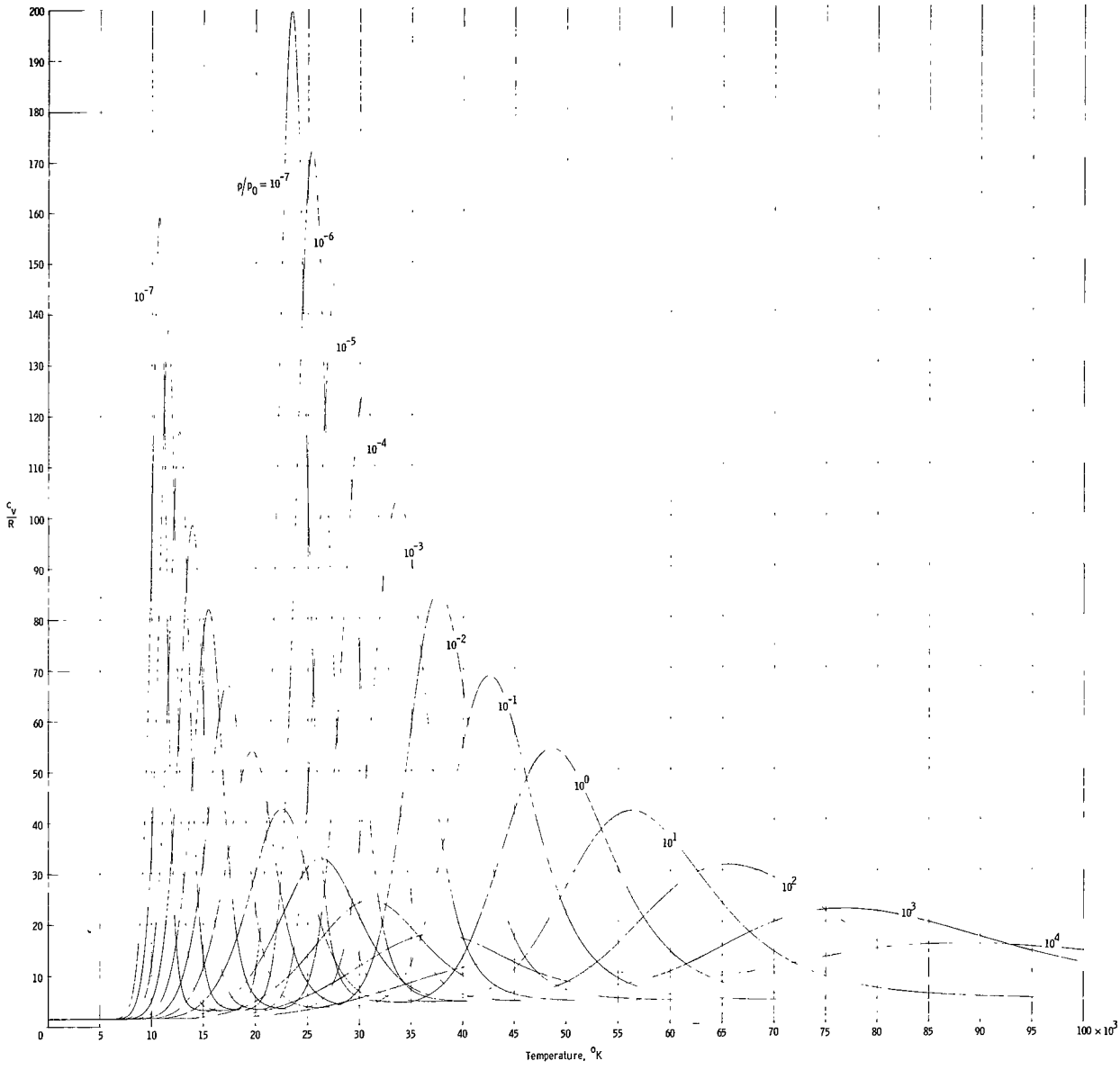

Figure 10.- Specific heat at constant volume of helium.

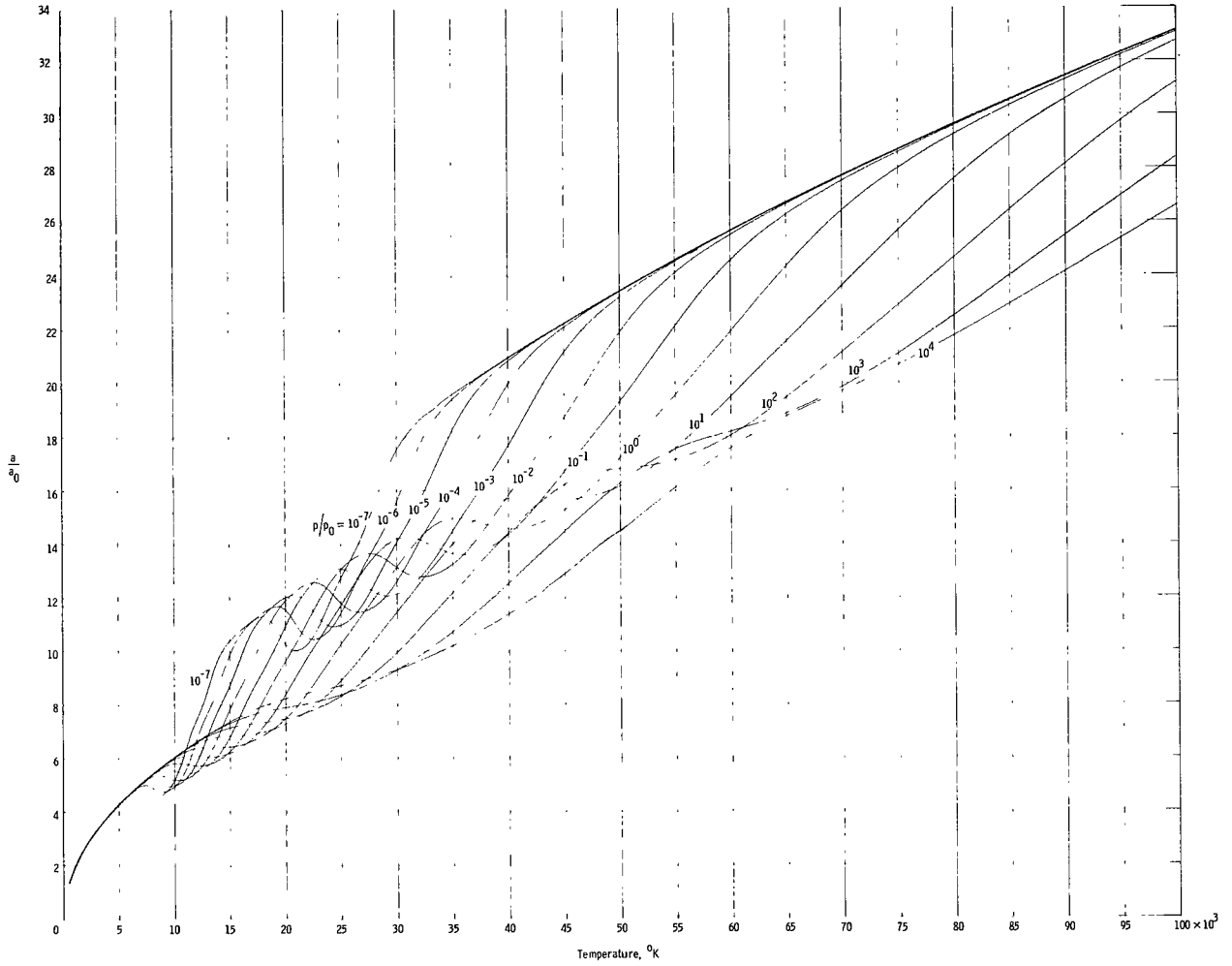

Figure 11.- Speed of sound in helium.

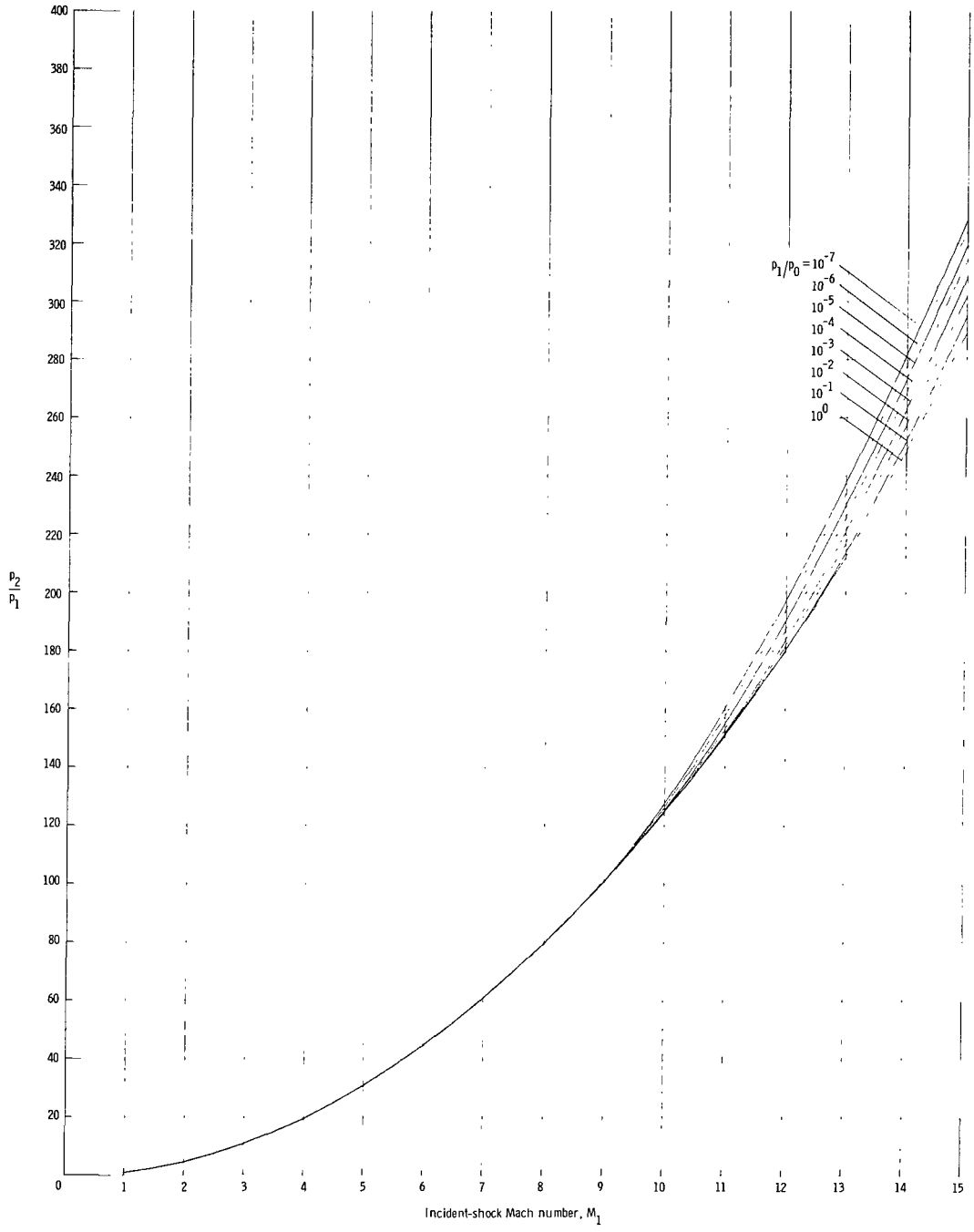

(a) $M_1 = 0$ to $M_1 = 15$.

Figure 12.- Pressure ratio behind the incident shock.

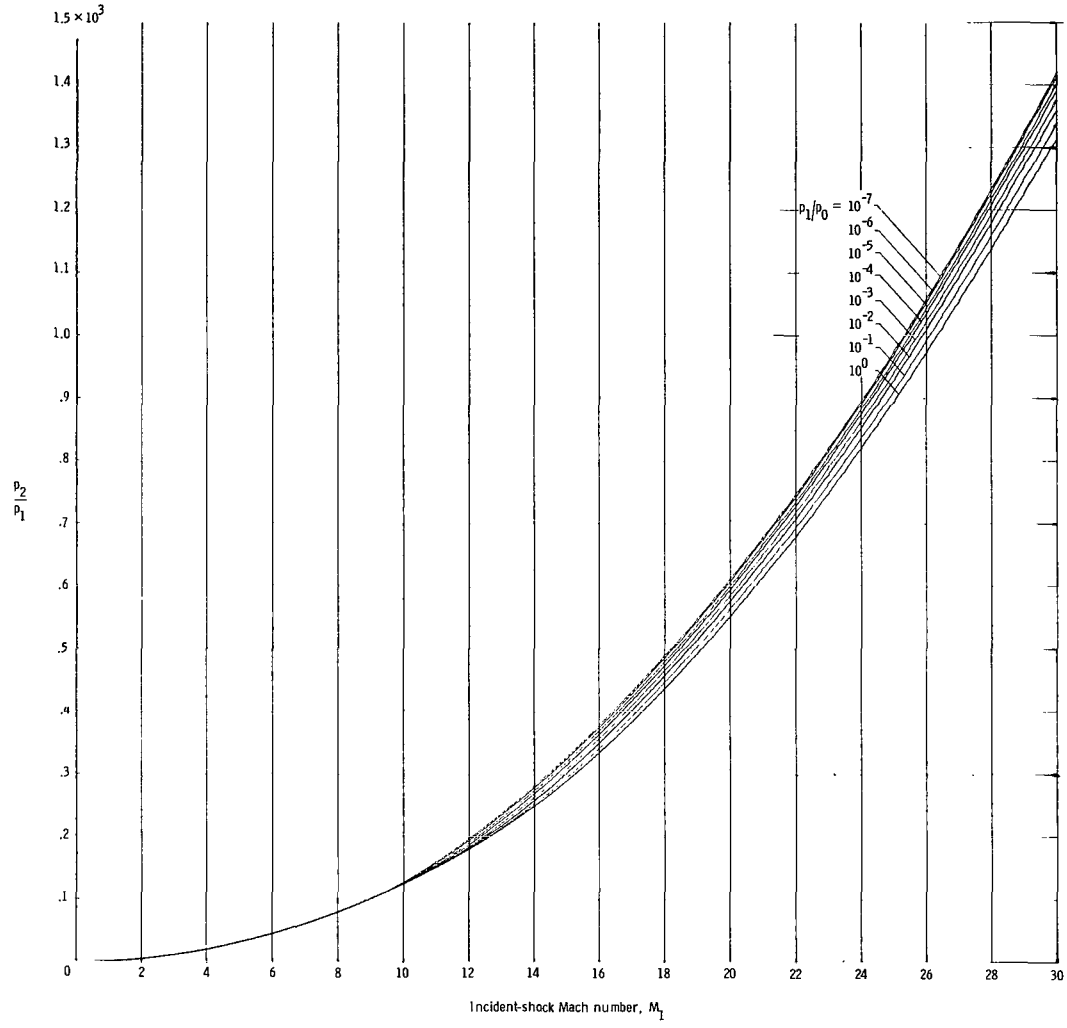

(b) $M_1 = 0$ to $M_1 = 30$.

Figure 12.- Concluded.

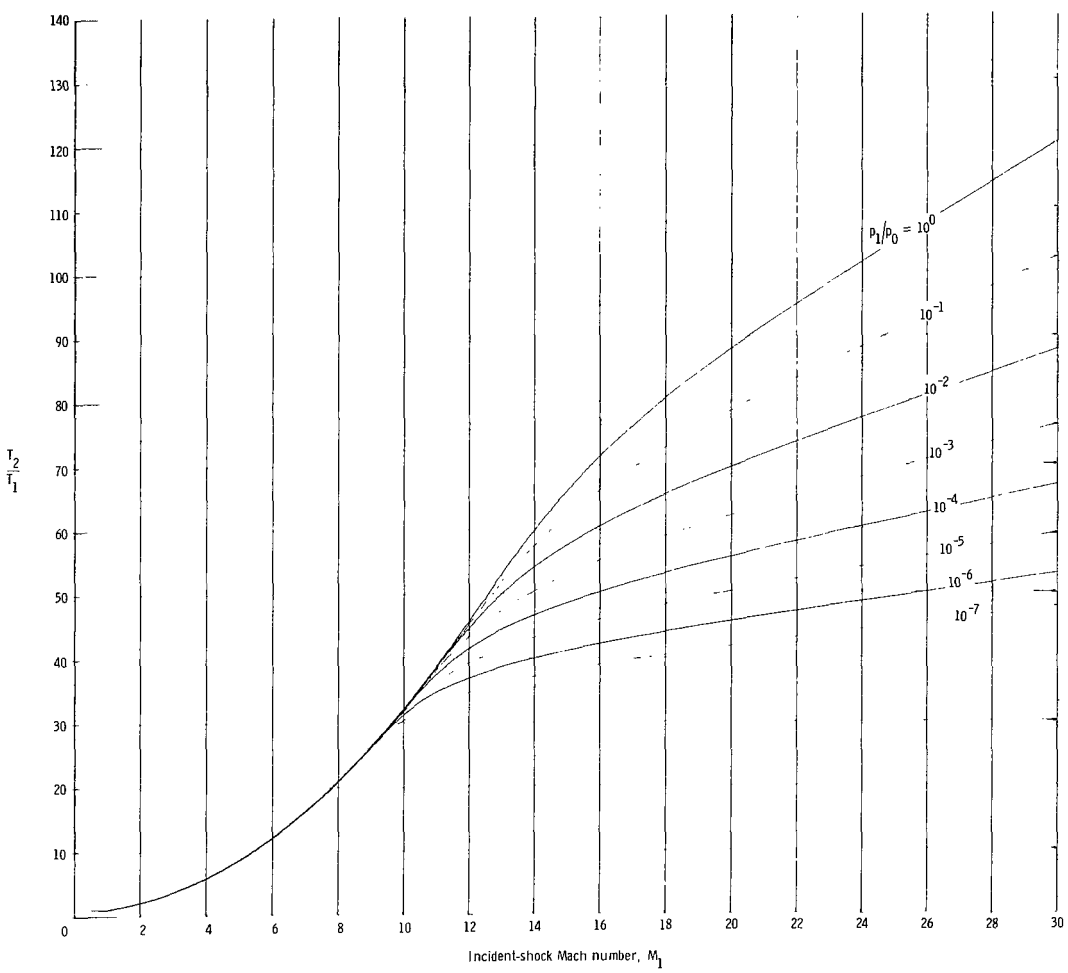

Figure 13.- Temperature ratio behind the incident shock.

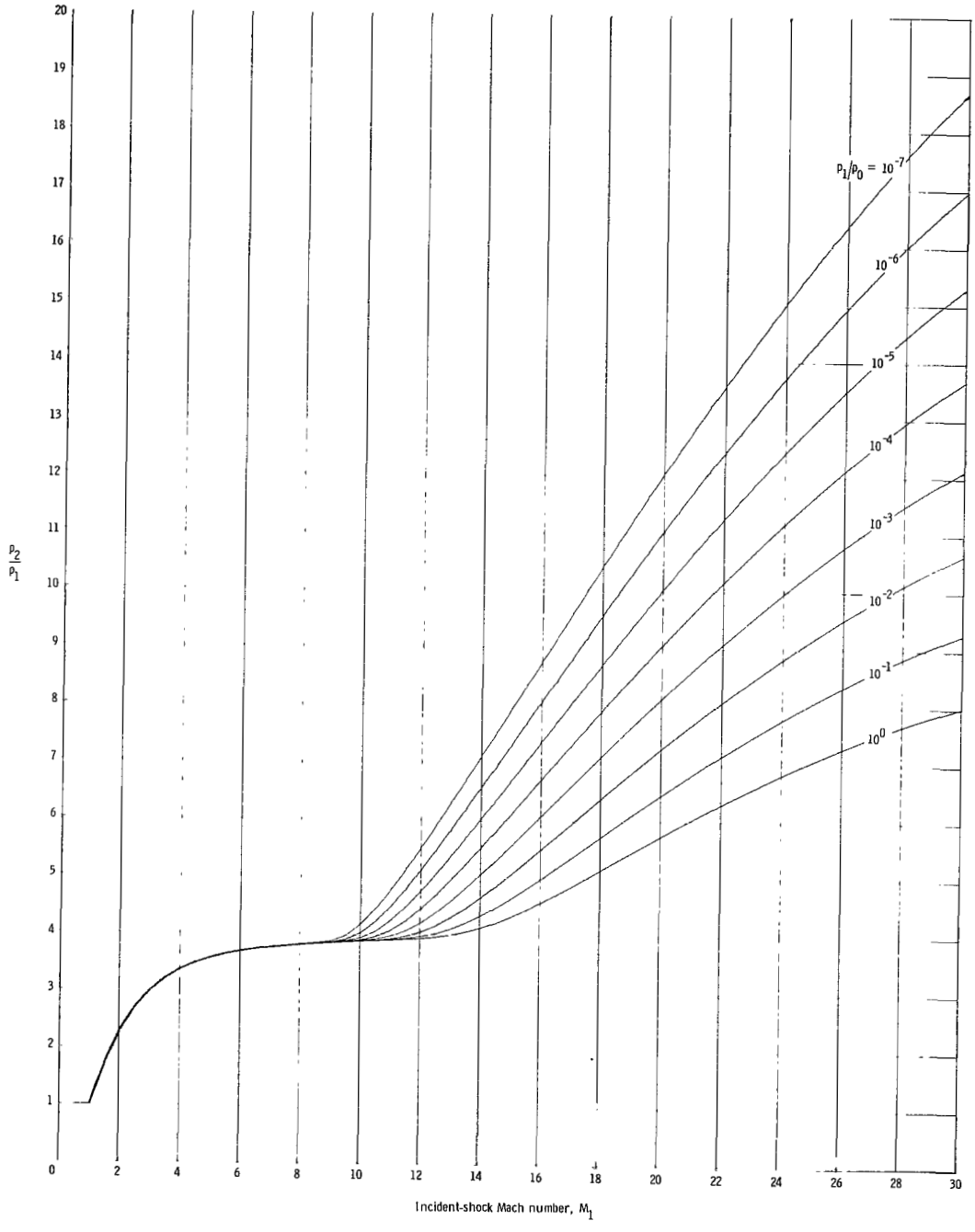

Figure 14.- Density ratio behind the incident shock.

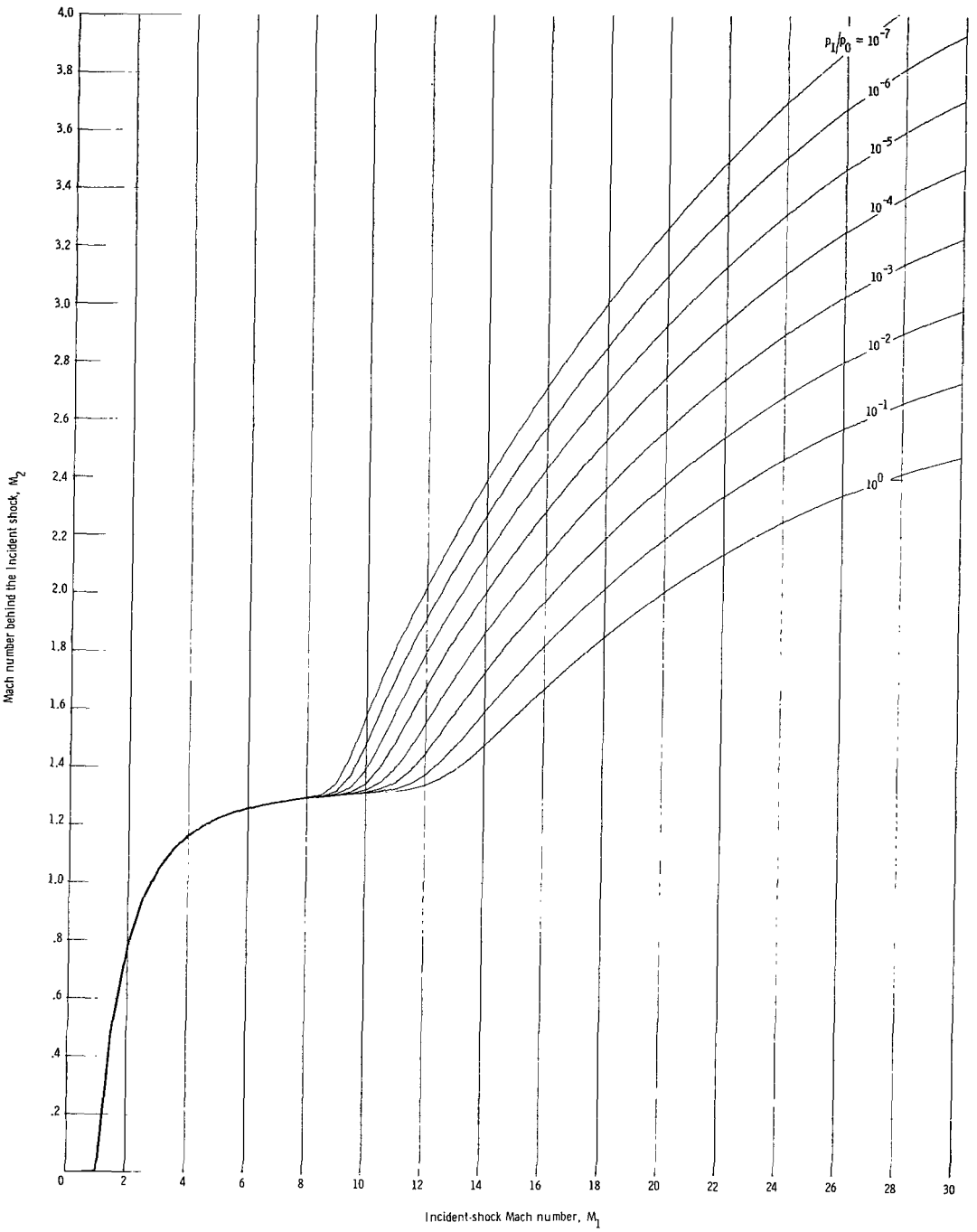

Figure 15.- Mach number behind the incident shock.

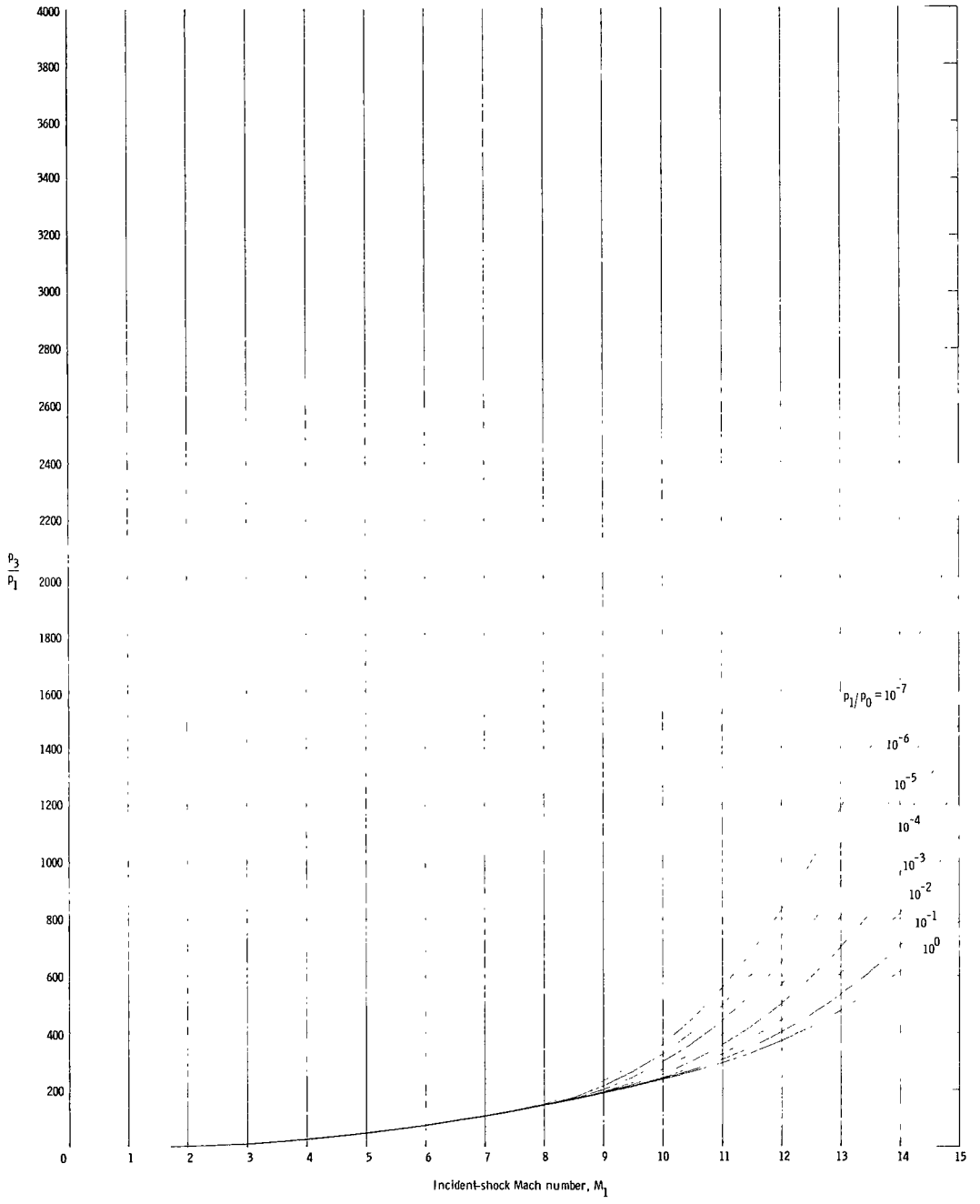

(a) $M_1 = 0$ to $M_1 = 15$.

Figure 16.- Pressure ratio behind the standing shock.

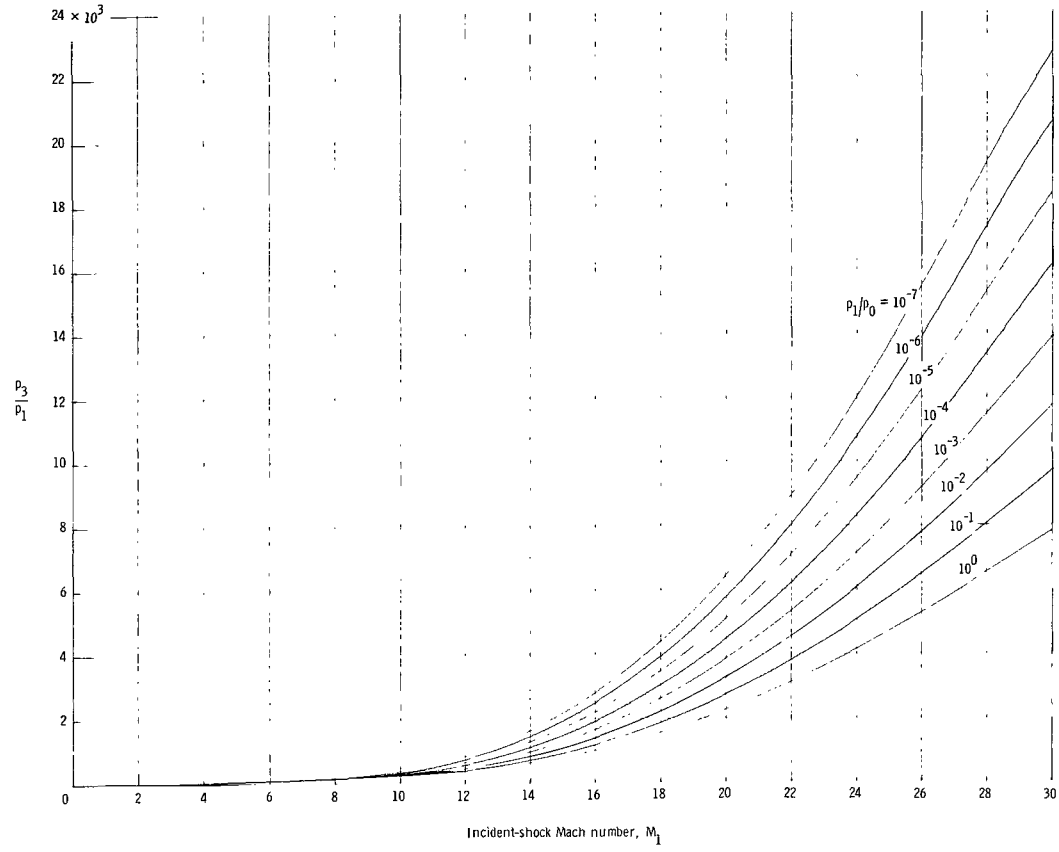

(b) $M_1 = 0$ to $M_1 = 30$.

Figure 16.- Concluded.

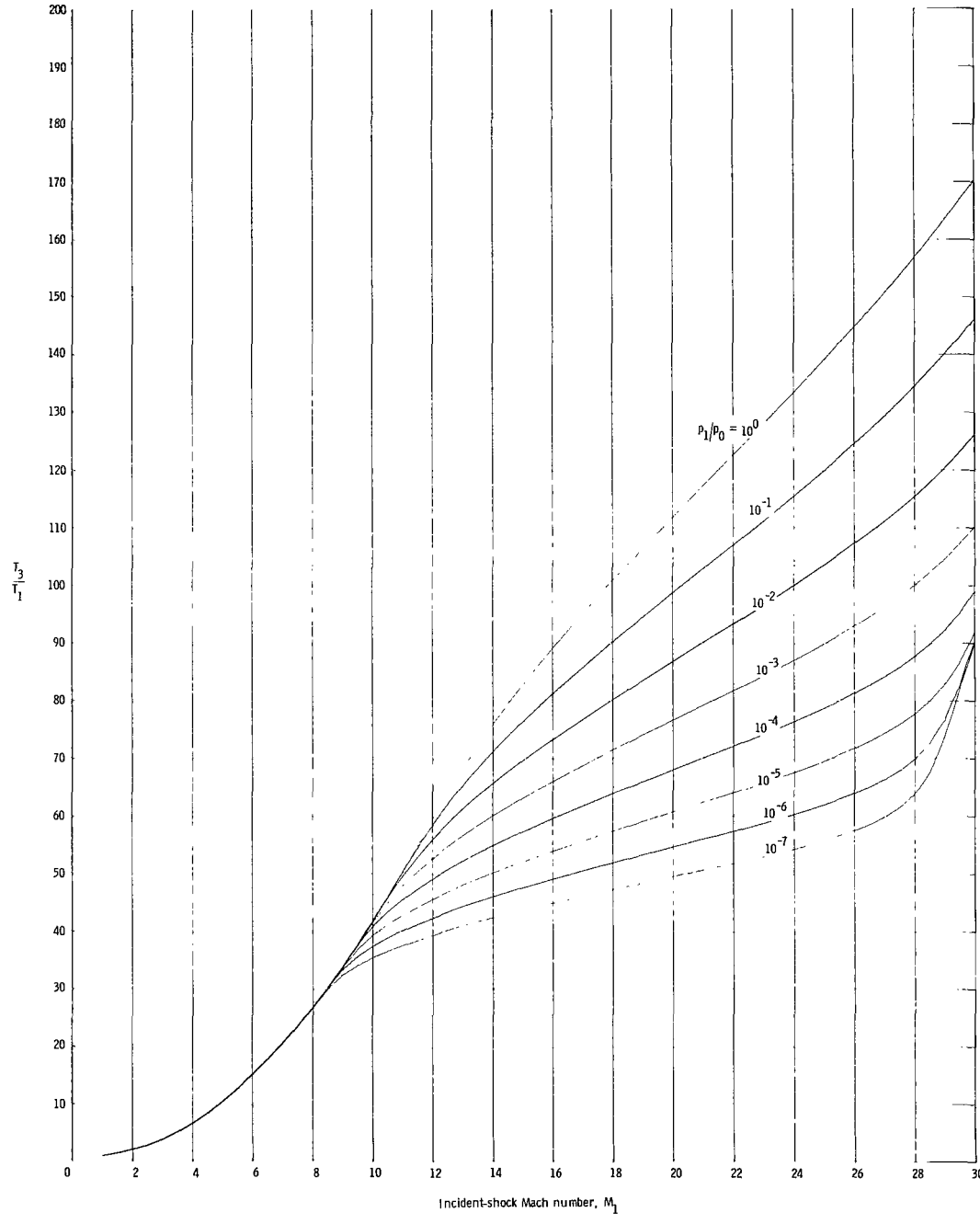

Figure 17.- Temperature ratio behind the standing shock.

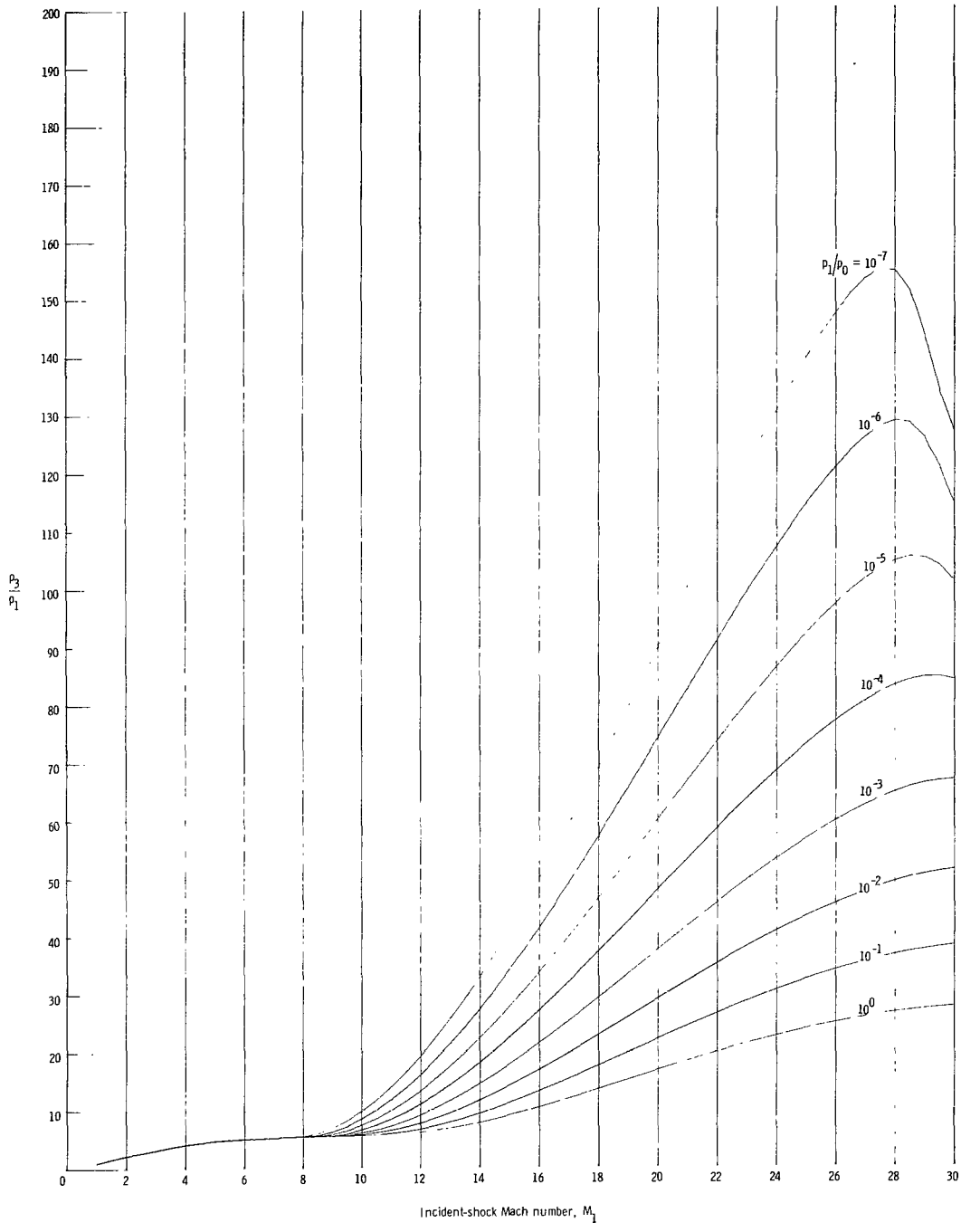

Figure 18.- Density ratio behind the standing shock.

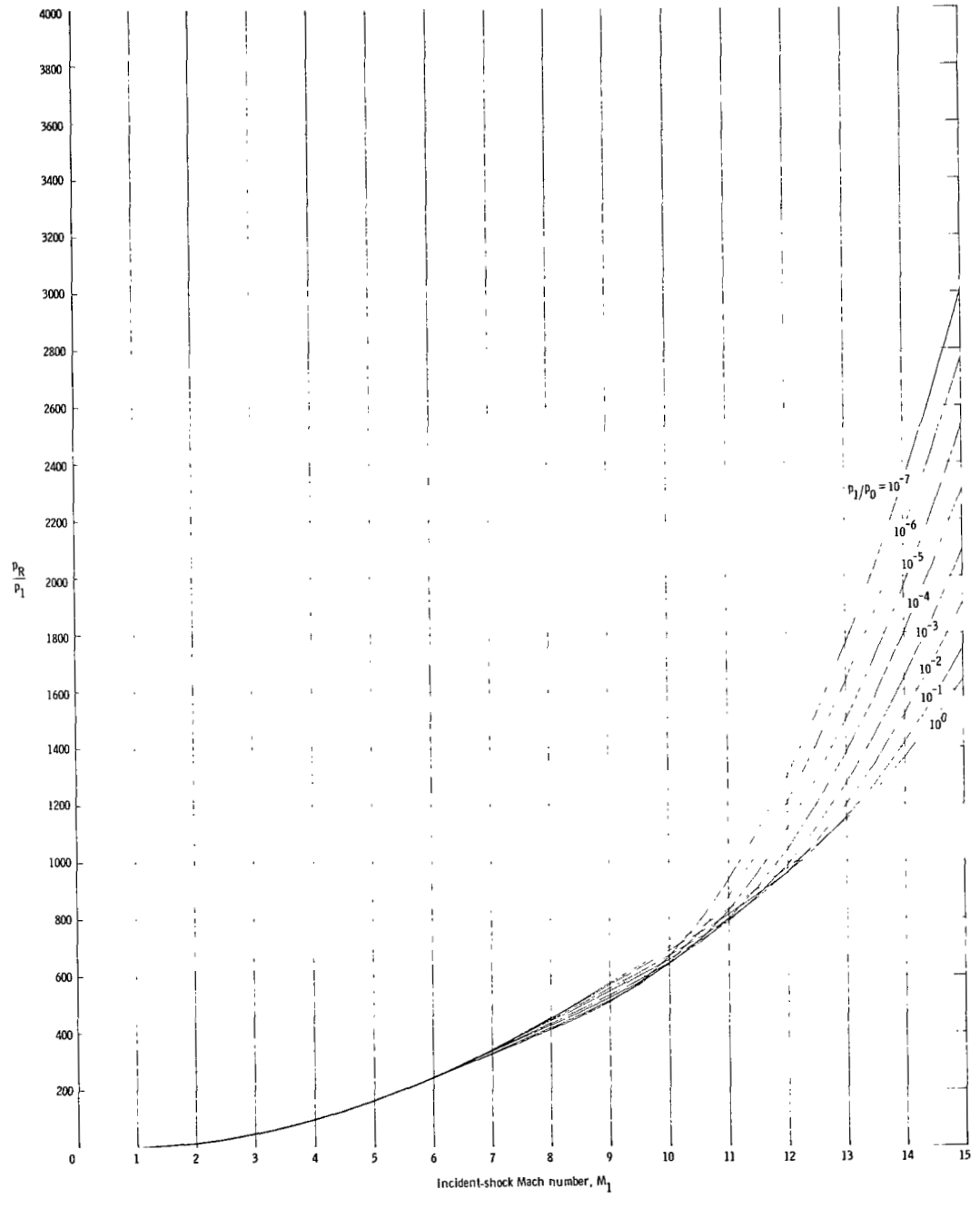

(a) $M_1 = 0$ to $M_1 = 15$.

Figure 19.- Pressure ratio behind the reflected shock.

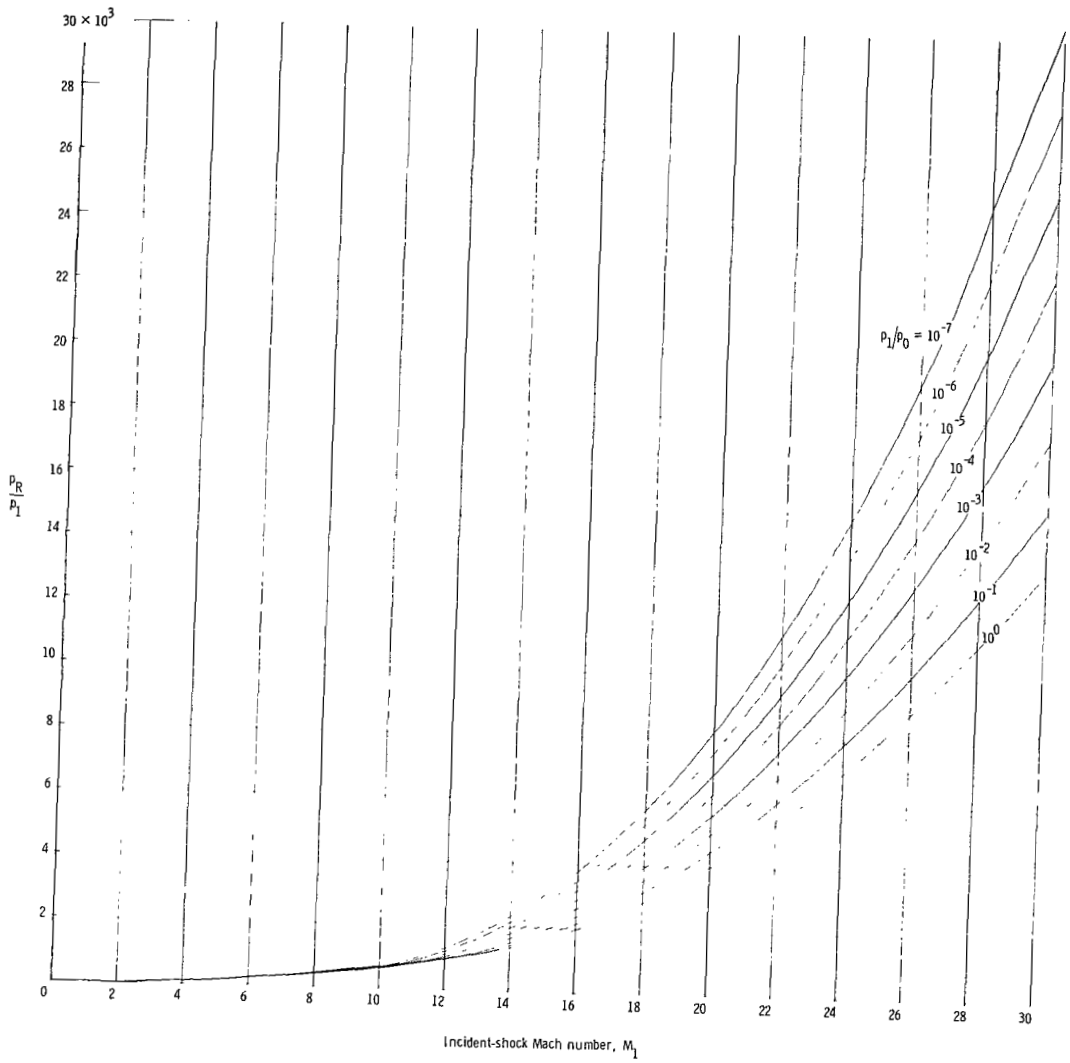

(b) $M_1 = 0$ to $M_1 = 30$.

Figure 19.- Concluded.

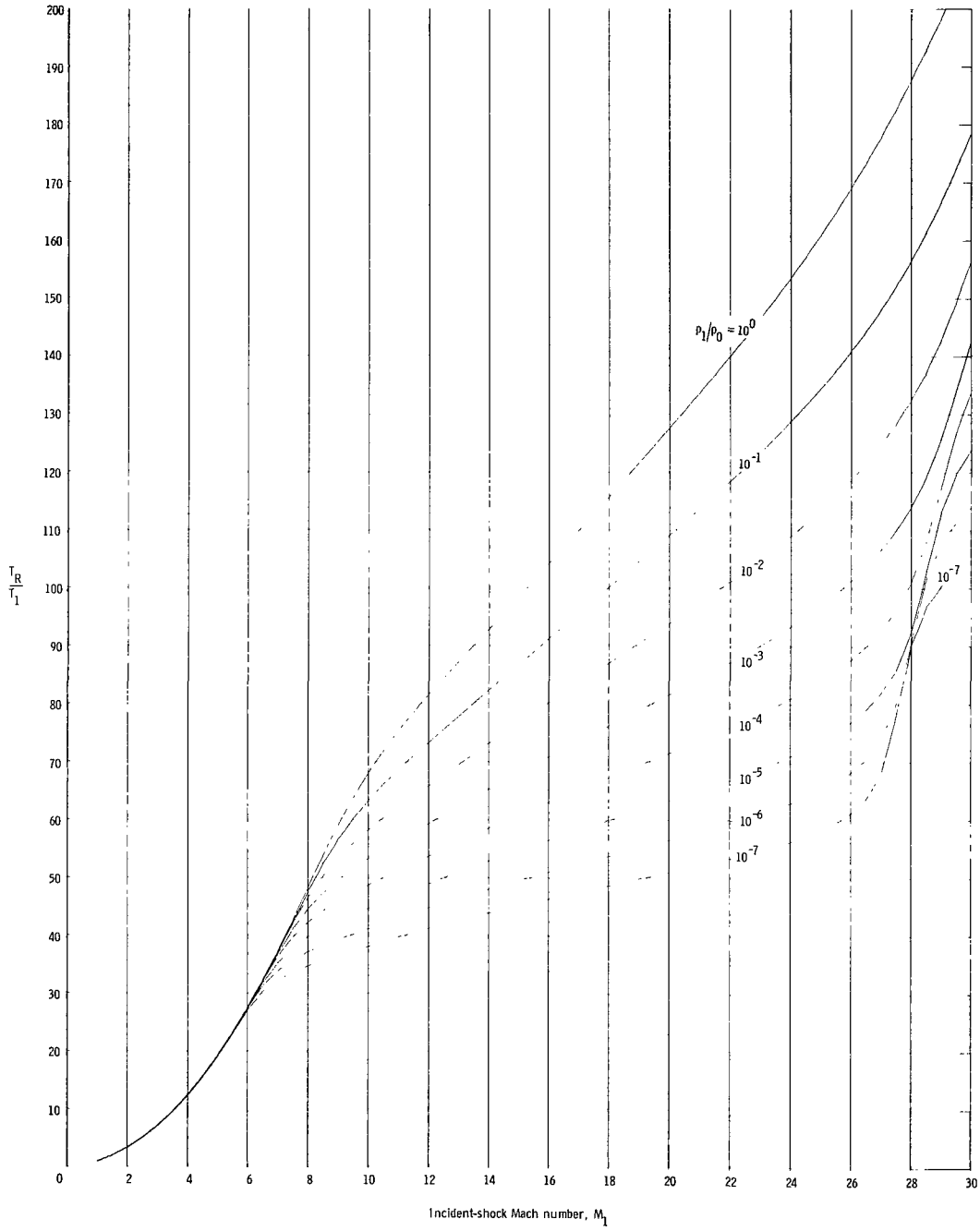

Figure 20.- Temperature ratio behind the reflected shock.

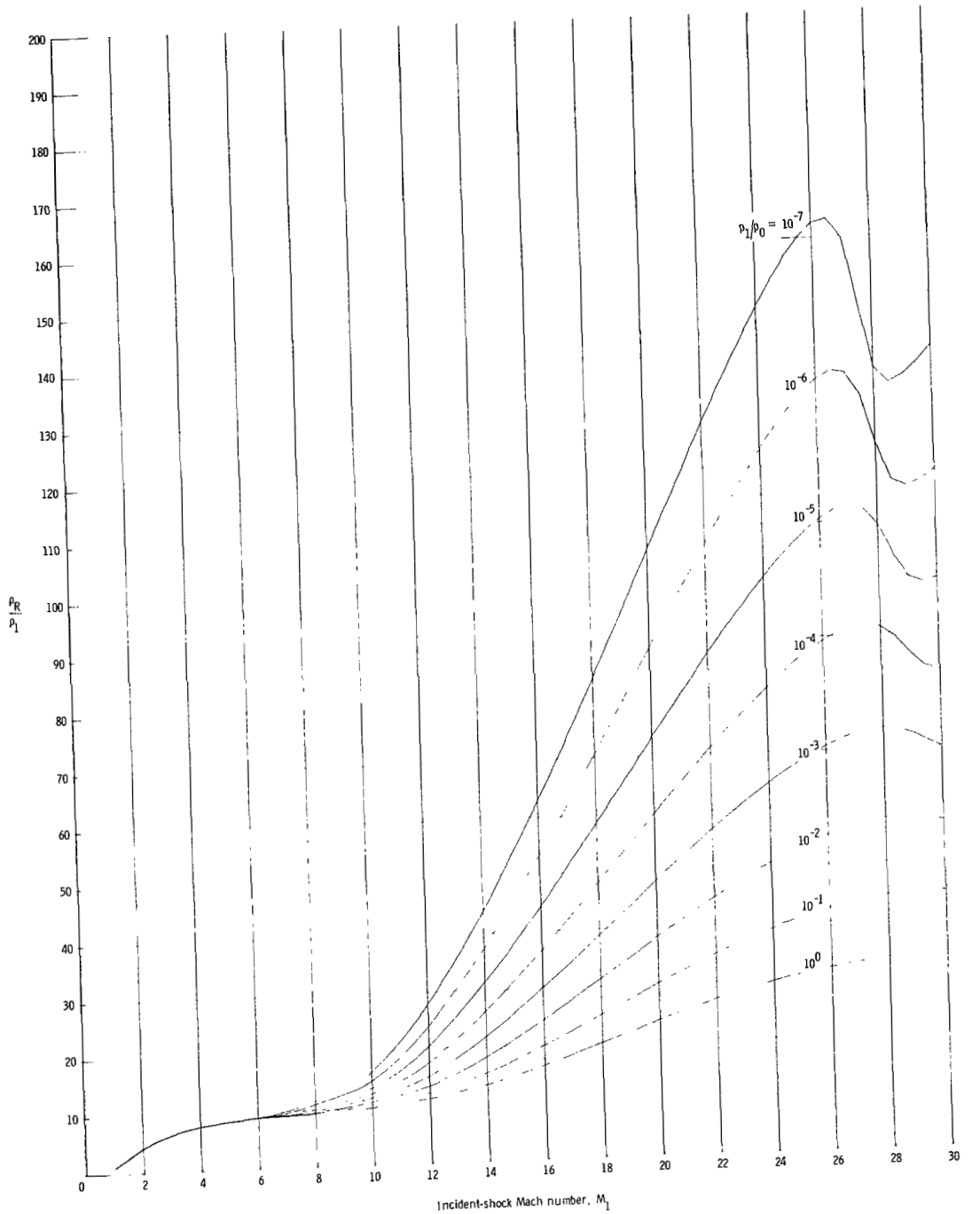

Figure 21.- Density ratio behind the reflected shock.

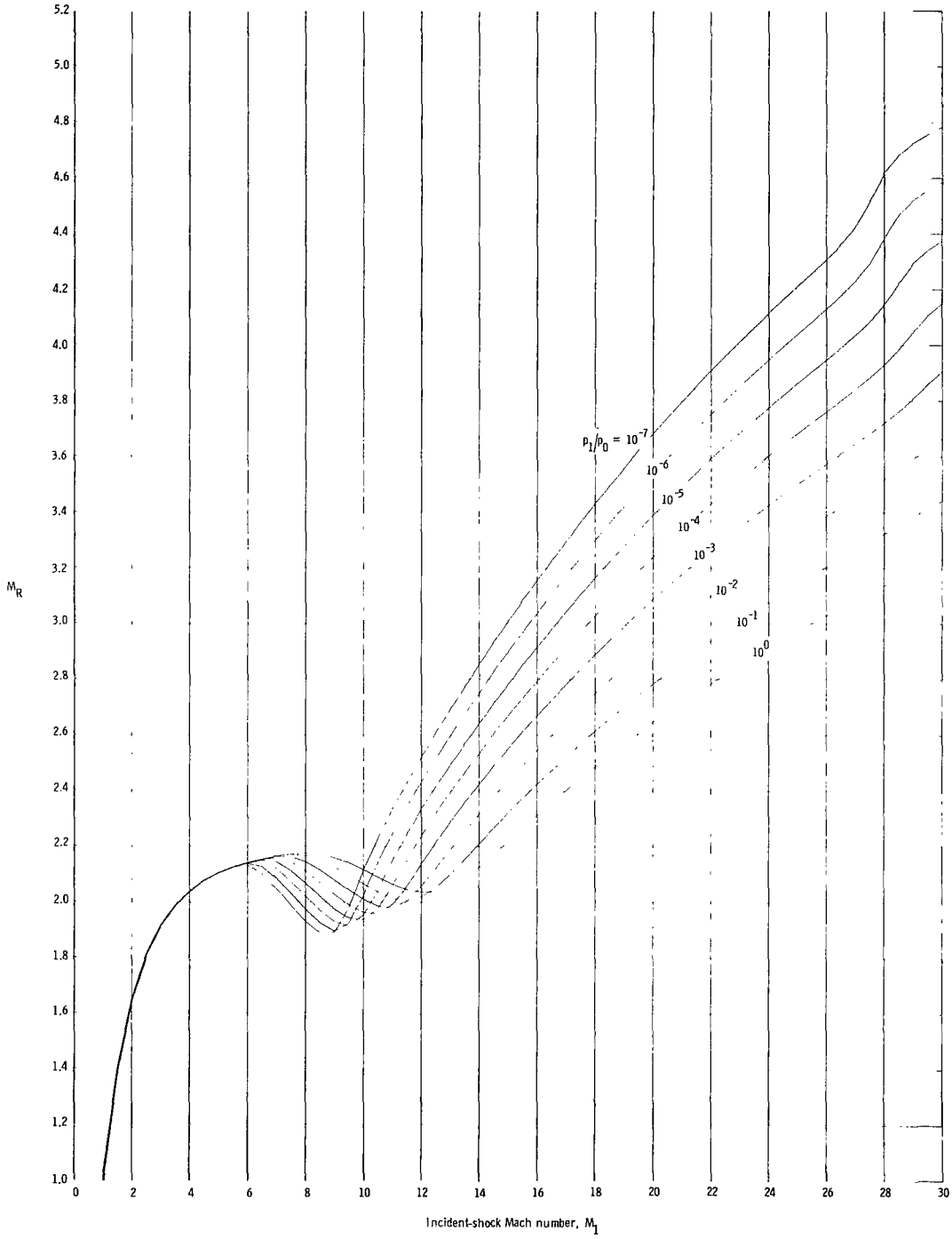

Figure 22.- Mach number of the reflected shock.

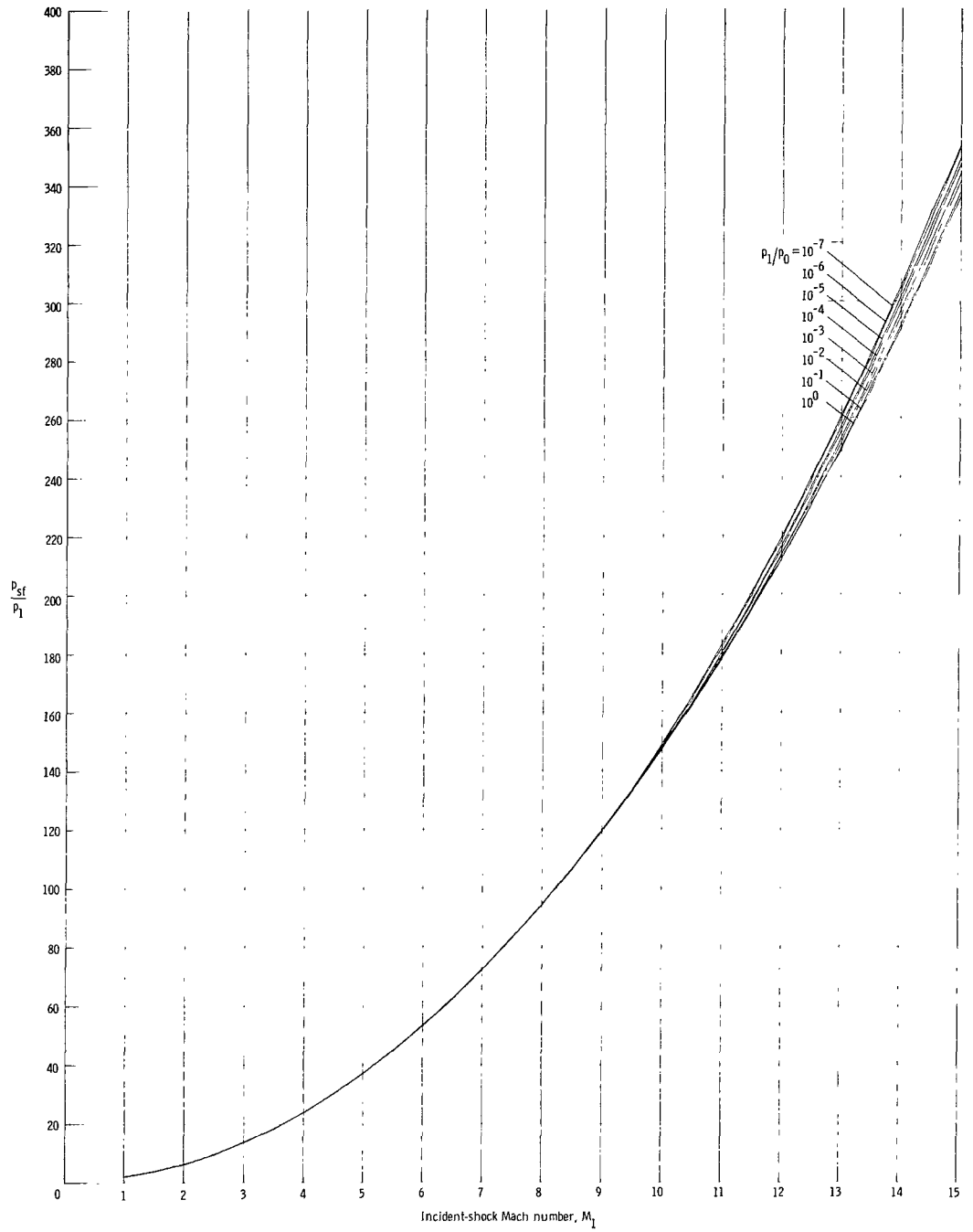

(a) $M_1 = 0$ to $M_1 = 15$.

Figure 23.- Pressure ratio at the in-flight stagnation point.

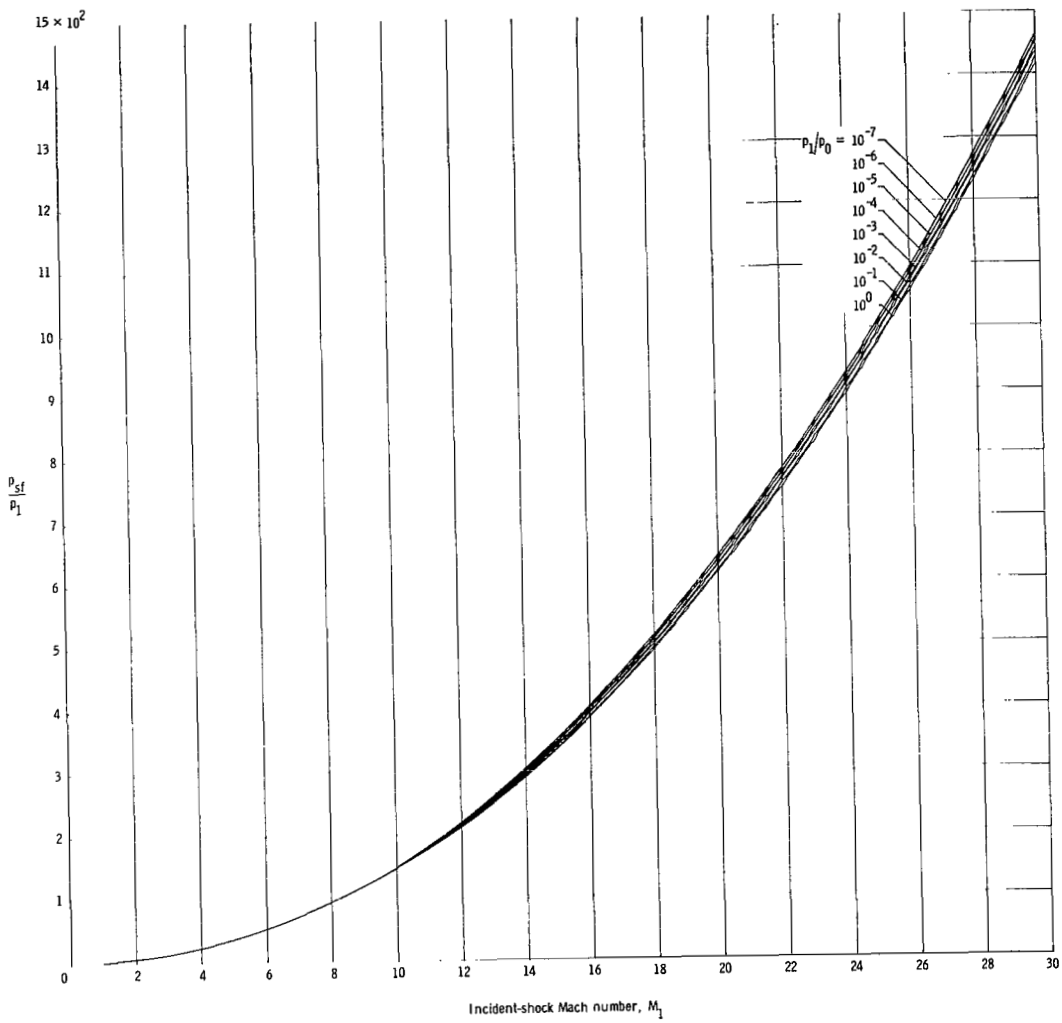

(b) $M_1 = 0$ to $M_1 = 30$.

Figure 23.- Concluded.

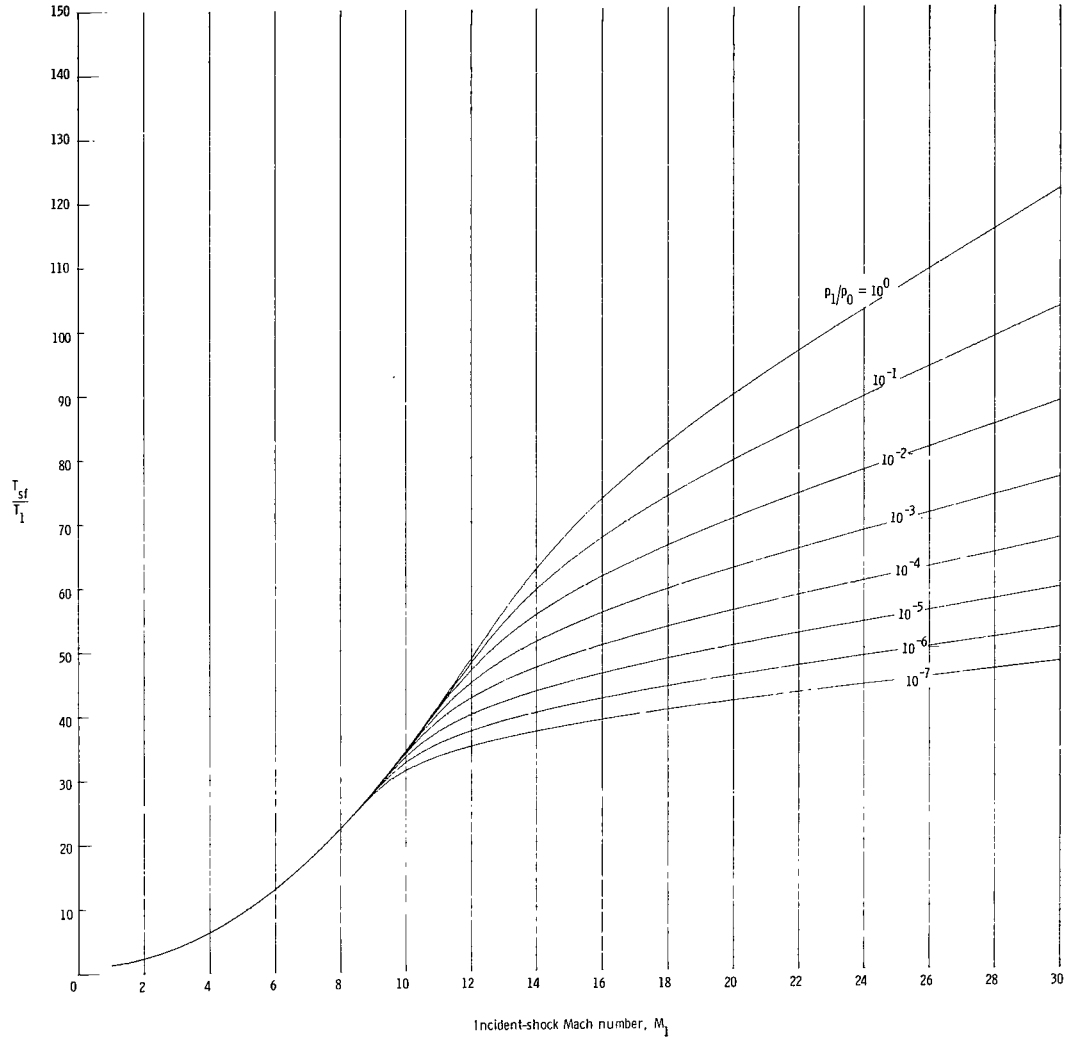

Figure 24.- Temperature ratio at the in-flight stagnation point.

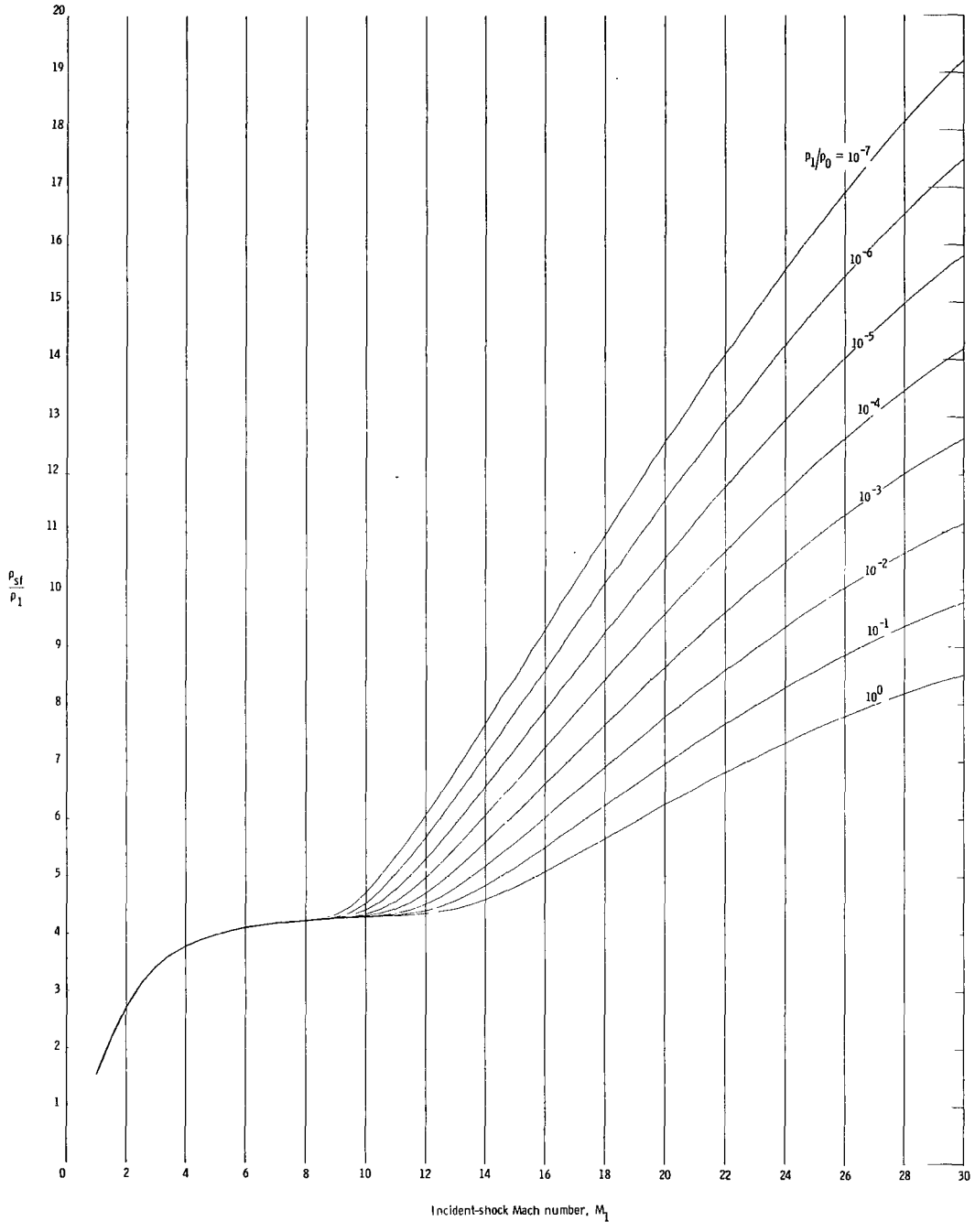

Figure 25.- Density ratio at the in-flight stagnation point.

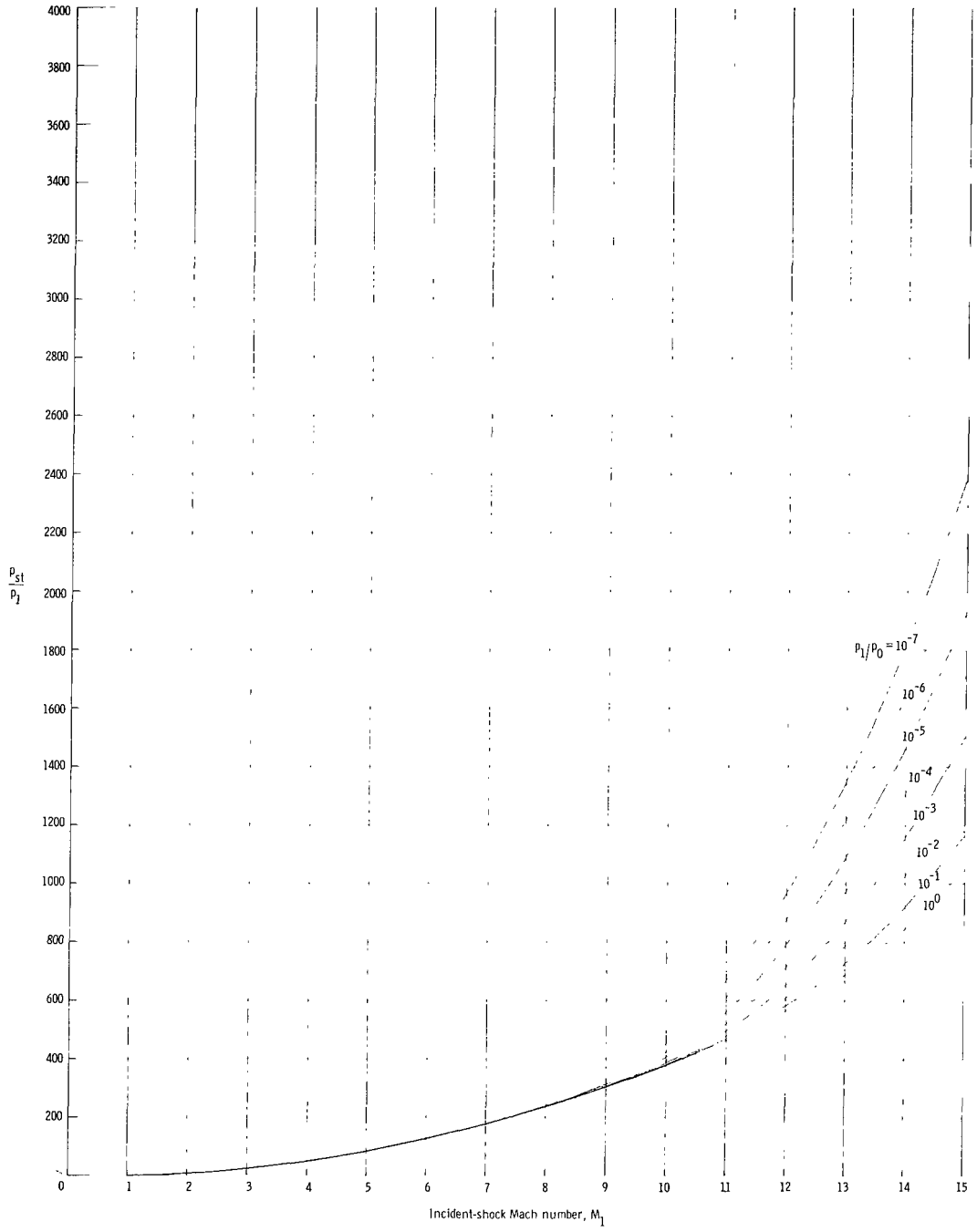

(a) $M_1 = 0$ to $M_1 = 15$.

Figure 26.- Pressure ratio at the shock-tube stagnation point.

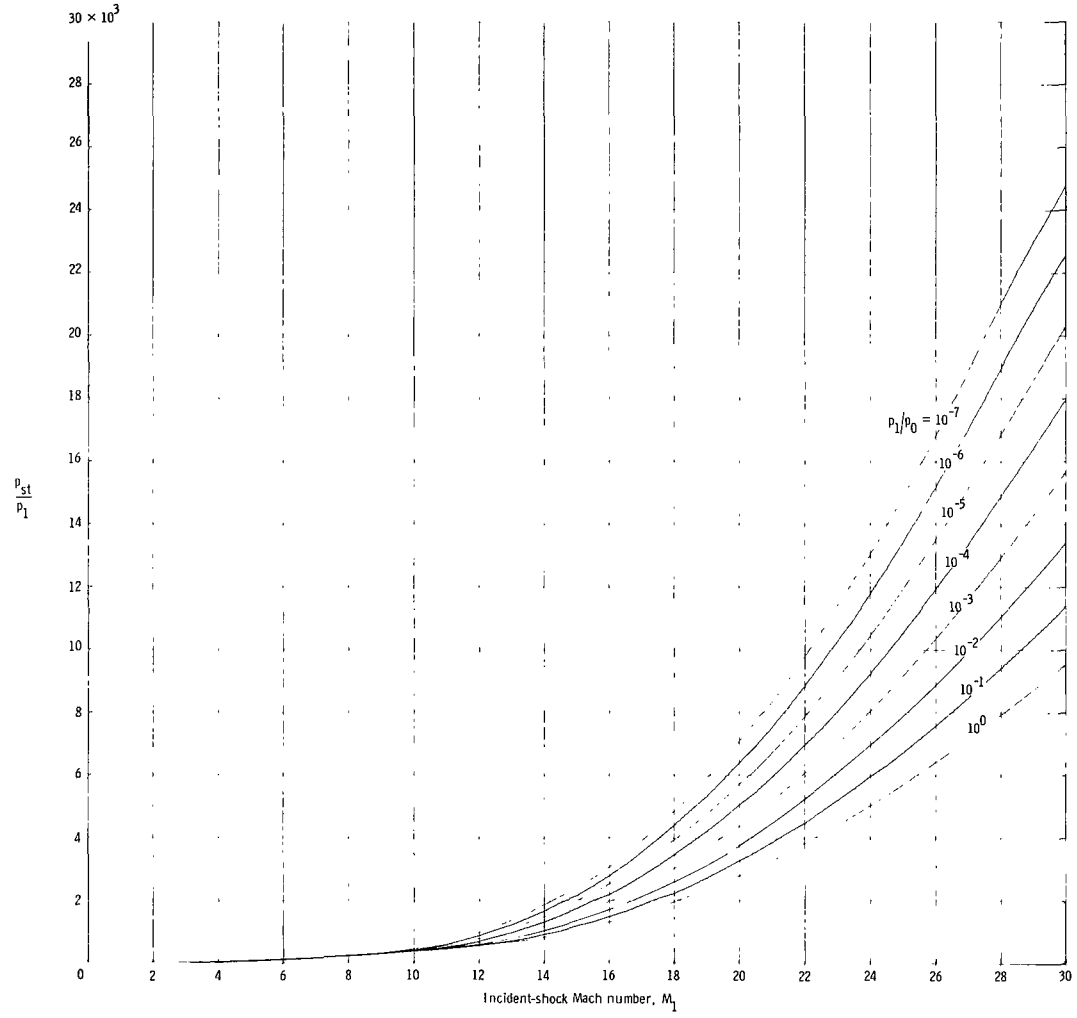

(b) $M_1 = 0$ to $M_1 = 30$.

Figure 26.- Concluded.

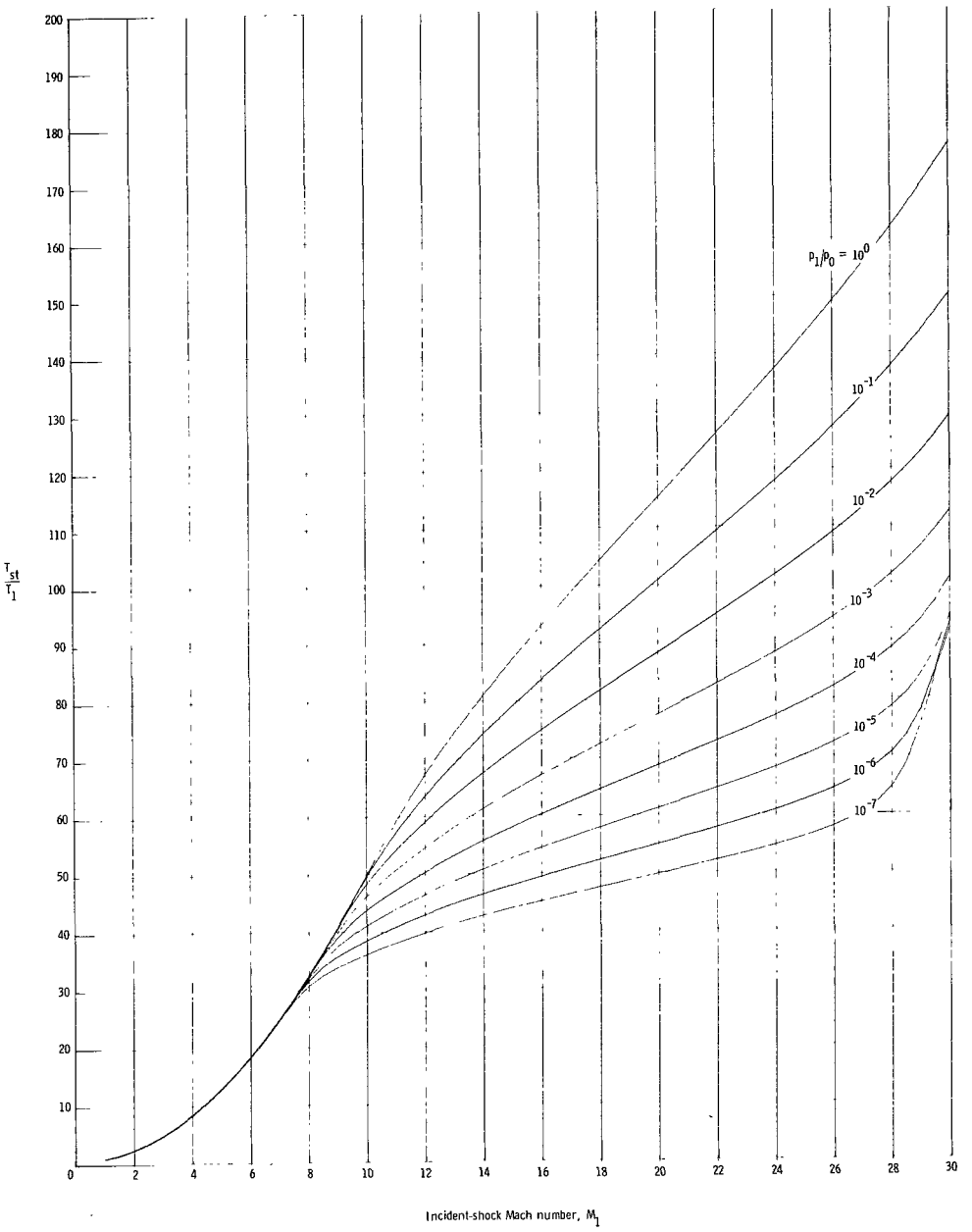

Figure 27.- Temperature ratio at the shock-tube stagnation point.

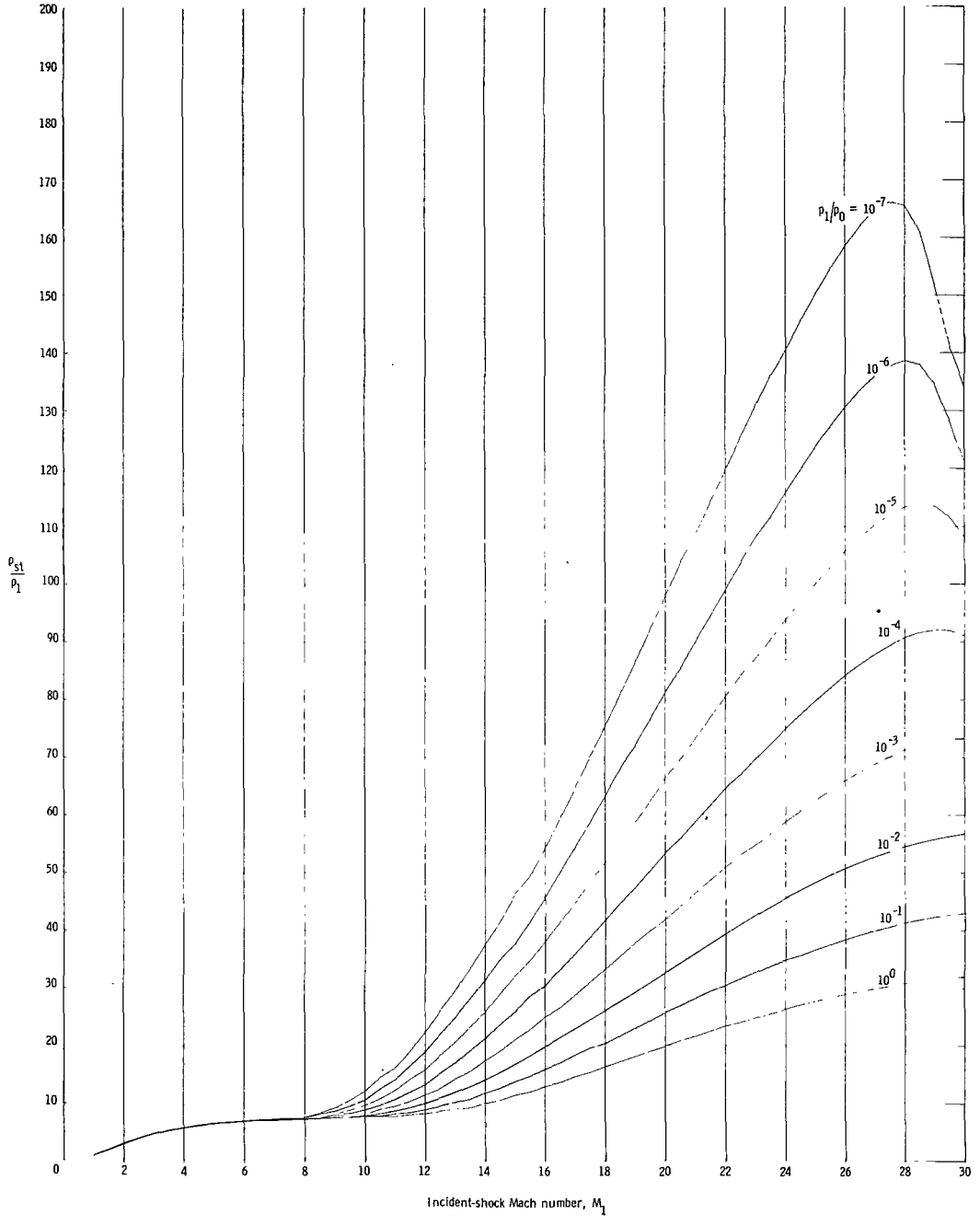

Figure 28.- Density ratio at the shock-tube stagnation point.

"The aeronautical and space activities of the United States shall be conducted so as to contribute . . . to the expansion of human knowledge of phenomena in the atmosphere and space. The Administration shall provide for the widest practicable and appropriate dissemination of information concerning its activities and the results thereof."

—NATIONAL AERONAUTICS AND SPACE ACT OF 1958

NASA SCIENTIFIC AND TECHNICAL PUBLICATIONS

TECHNICAL REPORTS: Scientific and technical information considered important, complete, and a lasting contribution to existing knowledge.

TECHNICAL NOTES: Information less broad in scope but nevertheless of importance as a contribution to existing knowledge.

TECHNICAL MEMORANDUMS: Information receiving limited distribution because of preliminary data, security classification, or other reasons.

CONTRACTOR REPORTS: Scientific and technical information generated under a NASA contract or grant and considered an important contribution to existing knowledge.

TECHNICAL TRANSLATIONS: Information published in a foreign language considered to merit NASA distribution in English.

SPECIAL PUBLICATIONS: Information derived from or of value to NASA activities. Publications include conference proceedings, monographs, data compilations, handbooks, sourcebooks, and special bibliographies.

TECHNOLOGY UTILIZATION PUBLICATIONS: Information on technology used by NASA that may be of particular interest in commercial and other non-aerospace applications. Publications include Tech Briefs, Technology Utilization Reports and Notes, and Technology Surveys.

Details on the availability of these publications may be obtained from:

SCIENTIFIC AND TECHNICAL INFORMATION DIVISION

NATIONAL AERONAUTICS AND SPACE ADMINISTRATION

Washington, D.C. 20546